FNP

JOURNAL OF FOOD PROCESS ENGINEERING

D.R. HELDMAN
and
R.P. SINGH
COEDITORS

FOOD & NUTRITION PRESS, INC.

OLUME 14, NUMBER 4

QUARTERLY

JOURNAL OF FOOD PROCESS ENGINEERING

All articles for publication and inquiries regarding publication should be sent to DR. D.R. HELDMAN, COEDITOR, *Journal of Food Process Engineering,* National Food Processors Association, 1401 New York Ave., N.W., Washington, D.C. 20005 USA: or DR. R.P. SINGH, COEDITOR, *Journal of Food Process Engineering,* University of California, Davis, Department of Agricultural Engineering, Davis, CA 95616 USA.

All subscriptions and inquiries regarding subscriptions should be sent to Food & Nutrition Press, Inc., 2 Corporate Drive, P.O. Box 374, Trumbull, CT 06611 USA.

One volume of four issues will be published annually. The price for Volume 14 is $104.00 which includes postage to U.S., Canada, and Mexico. Subscriptions to other countries are $123.00 per year via surface mail, and $132.00 per year via airmail.

Subscriptions for individuals for their own personal use are $84.00 for Volume 14 which includes postage to U.S., Canada, and Mexico. Personal subscriptions to other countries are $103.00 per year via surface mail, and $112.00 per year via airmail. Subscriptions for individuals should be sent direct to the publisher and marked for personal use.

The *Journal of Food Process Engineering* (ISSN: 0145-8876) is published quarterly (March, June, September and December) by Food & Nutrition Press, Inc.—Office of Publication is 2 Corporate Drive, P.O. Box 374, Trumbull, Connecticut 06611 USA. (Current issue is December, 1991.)

Second class postage paid at Bridgeport, CT 06602.

POSTMASTER: Send address changes to Food & Nutrition Press, Inc., 2 Corporate Drive, P.O. Box 374, Trumbull, CT 06611.

RENEWAL INVOICE

Payment must accompany this Renewal Invoice

Journal of FOOD PROCESS ENGINEERING

FTH289JFEV13V14
DIV SCI & TECH INFO
DEPT OF SCIENCE SVCE
RAMA VI ST
BANGKOK 10400 THAILAND

Your subscription is due for renewal.
To avoid interruption in service or missing issues, please fill in and mail this form with your payment now.

15	—— 1 year	$120.00
15 & 16	—— 2 years	$230.00
15, 16 & 17	—— 3 years	$345.00

Outside the U.S., Canada & Mexico, please add $19.00 per year for surface shipment, or $28.00 per year for air shipment.

PLEASE RENEW

YOUR SUBSCRIPTION HAS EXPIRED

Food & Nutrition Press, Inc.
2 Corporate Drive
P.O. Box 374
Trumbull, Connecticut 06611 USA

Tel. (203)261-8587
FAX(203)261-9724

JOURNAL OF FOOD PROCESS ENGINEERING

JOURNAL OF FOOD PROCESS ENGINEERING

Journal of FOOD PROCESS ENGINEERING

VOLUME 14
NUMBER 4

Coeditors: D.R. HELDMAN
R.P. SINGH

FOOD & NUTRITION PRESS, INC.
TRUMBULL, CONNECTICUT 06611 USA

ISSN 0145-8876

Printed in the United States of America

CONTENTS

EQUILIBRIUM DATA FOR OSMOTIC CONCENTRATION OF POTATO IN NACL-WATER SOLUTION

R. N. BISWAL[1,2,3] and K. BOZORGMEHR[1]

[1]*Department of Food Technology & Science*
[2]*Department of Agricultural Engineering*
The University of Tennessee
Knoxville, TN

Accepted for Publication July 25, 1991

ABSTRACT

Equilibrium data needed in modeling of osmotic dehydration are reported for unblanched diced potato in contact with aqueous solutions of sodium chloride. Diced potato, 1 cm cubes, were equilibrated with 0–12% (w/w) aqueous NaCl solutions at three temperatures (8, 21 and 35°C). The mass fraction of total solids nonsalt (w_3^*) in potato at equilibrium was modeled as a function of mass fraction of total solids in the fresh material at full turgor (w_3^F), concentration of NaCl in the external solution (w_{1B}) and temperature. Using w_3^* and w_{1B}, and assuming that the activity of NaCl in the potato tissue and the external solution at equilibrium are equal, equilibrium densities were calculated based on the principle of volume additivity. The predicted and experimentally measured equilibrium densities were in close agreement.

INTRODUCTION

Osmotic dehydration is defined as a process in which part of the natural moisture in plant materials is removed by immersion in aqueous solutions of sucrose, glucose, fructose, sodium chloride or other osmotic agents. As moisture is removed, soluble solids in solution penetrate the material, and some soluble solids present in the material may leach out (Ponting *et al.* 1966; Biswal *et al.* 1991.

Osmotic dehydration has been applied to concentrating fruits and vegetables prior to freeze dehydration (Hawkes and Flink 1978), air drying (Kim and Toledo 1987) and freezing (Torreggiani *et al.* 1988; Biswal and Bozorgmehr 1989). In

[3]Correspondence: Dr. R. N. Biswal, Department of Food Technology & Science, The University of Tennessee, P.O. Box 1071, Knoxville, TN 37901-1071; Phone (615) 974-7334.

Journal of Food Process Engineering **14** (1991) 237-245.

addition to reducing process energy requirements, osmotic dehydration has been shown to improve product quality (Hawkes and Flink 1978). A comprehensive review of the osmotic dehydration process is given by Le Maguer (1988).

To date, more work has been done on osmotic dehydration of fruit than vegetable tissues. The potato is one vegetable tissue that several researchers have successfully concentrated by osmotic means in recent years. The feasibility of obtaining dehydrofrozen potato by osmotic means was demonstrated by Hartal (1967). End point criteria for osmosis and the spatial distribution of the osmotic effect (water and solute concentrations) in potato tissue in contact with aqueous solutions of sodium chloride and sucrose were studied by Lenart and Flink (1984a,b). Osmotically induced mass transfer in potato and other plant storage tissue was studied by Toupin and Le Maguer (1989) and Toupin *et al.* (1989). Recently, Barcenas *et al.* (1990) obtained the diffusional parameters for osmotic dehydration of potato in aqueous solutions of sodium chloride.

Modeling the kinetics of osmosis for concentrating vegetable tissue would require data on surface properties of the material in contact with the osmotic solution. Examples of these properties are composition and density of the material at the surface. Assuming that surface of the tissue is in equilibrium with the contact solution, these properties can be obtained by equilibrating the whole tissue in the osmotic solution (Biswal and Le Maguer 1989).

Objectives of this research were to collect and to model the equilibrium data for osmotic concentration of potato in aqueous solutions of sodium chloride.

REVIEW OF THE MODEL

Biswal and Le Maguer (1989) reported that the system of diced potato soaked in aqueous solution of sodium chloride can be considered to consist of NaCl, water, and total solids nonsalt. Water and NaCl are the only components that are exchanged between diced potato and external solution, while the total solids nonsalt, present in potato, is assumed to remain constant (no leaching).

The concentration of NaCl or water in diced potato in equilibrium with an external solution of known composition, was calculated using the following equation as suggested by Biswal and Le Maguer (1989).

$$w_i^* = w_{iB}(1 - w_3^*) \tag{1}$$

In Eq. (1), the subscript i represents component 1 (salt) or 2 (water). B represents bath or external solution and superscript * represents equilibrium. Accordingly, w_3^* is the mass fraction of total solids nonsalt of the material in equilibrium with the external solution.

Neglecting the terms beyond quadratic, the model for w_3^*, as suggested by Biswal and Le Maguer (1989) is:

$$w_3^* = (A_0 + A_1 w_{1B} + A_2 w_{1B}^2)\, w_3^F$$

where $A_0 = B_0 + B_1 t + B_2 t^2$

$$A_1 = C_0 + C_1 t + C_2 t^2$$

$$A_2 = D_0 + D_1 t + D_2 t^2 \qquad (2)$$

w_{1B} = mass frac. of salt in the bath, kg NaCl/kg soln.

w_3^F = mass fraction of total solids-nonsalt (TSNS) in fresh material, kg TSNS/kg total.

t = contact temperature, °C

It should be mentioned that Eq. (1) is based on the assumption that the mean molal activity coefficients of sodium chloride in the material and the bath are equal. This assumption implies that the total solids nonsalt in the material act only as inert support.

MATERIALS AND METHODS

Osmotic solutions of 5%, 10%, and 15% NaCl by weight were prepared by mixing reagent grade sodium chloride in water. Two batches of large size Idaho white potatoes were obtained from a local produce market. Batch 1 potatoes were used to conduct one set of all experiments (replicate 1), and batch 2 potatoes were used for replicates 2 and 3. Potatoes were hand peeled and cut into 1 cm dices. The potato cubes were washed and standardized for initial moisture by soaking them in tap water for 1 h.

The diced potatoes were allowed to contact NaCl-water solutions at four concentrations (0%, 5%, 10% and 15% NaCl by weight) and three temperatures (8, 21 and 35°C) in flasks mounted in a constant temperature shaking bath. A solid:liquid ratio of 1:5 was maintained. Shaking the flasks produced good mixing of the potato cubes with the solution. Contact time was fixed at 24 h. Potato cubes were then removed from the solution, blotted dry and analyzed for reduction in mass; moisture (70°C under partial vacuum overnight); and salt by

titration (AOAC 1984). The final salt content of the osmotic solution was also measured by titration (AOAC 1984). Density of the potato cubes was measured in wide mouth pycnometers using hexane. All experiments were replicated three times.

RESULTS AND DISCUSSION

Equilibrium data (experimental) for diced potato in contact with aqueous solutions of sodium chloride are given in Table 1. At any given temperature, $(m_0,m_0)^*$.

TABLE 1
EQUILIBRIUM DATA FOR DICED POTATO IN CONTACT WITH NACL-WATER SOLUTIONS

Temperature (°C)	w_{1B}	m_e/m_0	w_1^*	w_3^*	ρ^* (kg/m³)
8(1)	Blank	-	-	0.1580	1061.8
	0.0	N/A	-	0.1330	1049.3
	0.0394	0.69	0.0276	0.2120	1115.6
	0.0768	0.77	0.0592	0.2150	1142.2
	0.1147	0.81	0.0775	0.190	1162.5
8(2)	Blank	-	-	0.176	N/A
	0.0	N/A	-	0.1444	N/A
	0.0427	0.66	0.0310	0.2224	1130.1
	0.0866	0.75	0.0620	0.1978	1148.6
	0.1246	0.78	0.0956	0.1731	1151.8
21(1)	Blank	-	-	0.1580	1061.8
	0.0	N/A	-	0.1386	1055.0
	0.0384	0.76	0.0382	0.1990	1103.0
	0.0817	0.79	0.0611	0.2073	1124.0
	0.1186	0.82	0.0856	0.1960	1134.0
21(2)	Blank	-	-	0.1761	N/A
	0.0	N/A	-	0.1583	N/A
	0.0407	0.70	0.0267	0.2031	1100.4
	0.0893	0.77	0.0645	0.1877	1125.7
	0.1264	0.80	0.0947	0.1723	1143.6
35(1)	Blank	-	-	0.1580	1061.8
	0.0	N/A	-	0.1610	1058.0
	0.0408	0.75	0.0257	0.2103	1149.5
	0.0782	0.80	0.0585	0.2180	1150.6
	0.1142	0.83	0.0920	0.1870	1146.2
35(2)	-		-	0.1761	N/A
	0.0	N/A	-	0.1815	N/A
	0.0407	0.76	0.0319	0.1898	1154.1
	0.0842	0.77	0.0630	0.2120	1148.1
	0.1246	0.78	0.0956	0.1731	1181.0

Number 1 in parentheses indicates replicate 1. Number 2 in parentheses indicates average of two replicates (replicates 2&3).

the mass ratio of potato at equilibrium relative to initial, increased as concentration of NaCl in external solution increased. The increased mass ratio is attributed to NaCl uptake by potato.

Published equilibrium data on potato/NaCl-water system is limited to Lenart and Flink's (1984a) work on Hansa potato in contact with 10% NaCl-water solution at 23°C. Solids gain (SG) and water loss (WL), calculated using Eqs. (1) and (2), respectively, of Lenart and Flink (1984a) was reported to be 5% and 20% of the original weight, respectively. In the present study, the closest condition to Lenart and Flink's (1984a) was 10% NaCl-water at 21°C. The average SG and WL calculated for this condition were 4% and 14% of the original weight, respectively. The differences in SG and WL values in both studies are attributed, to some extent, to the differences in contact temperature but greatly to the conditions of potato tissue used (varietal and storage condition differences).

As mentioned earlier, Eq. (1) was based on the assumption that at equilibrium the activities of NaCl in potato and the external solution are equal. This assumption was validated using w_1^* values calculated from Eq. (1) for each combination of w_{1B} and w_3^* (Table 1) and plotting (Fig. 1) against the experimental values of w_1^*. The close agreement between w_1^* (calculated) and w_1^* (experimental) (Fig. 1) validates the assumption of equality NaCl activities in potato and the external solution at equilibrium.

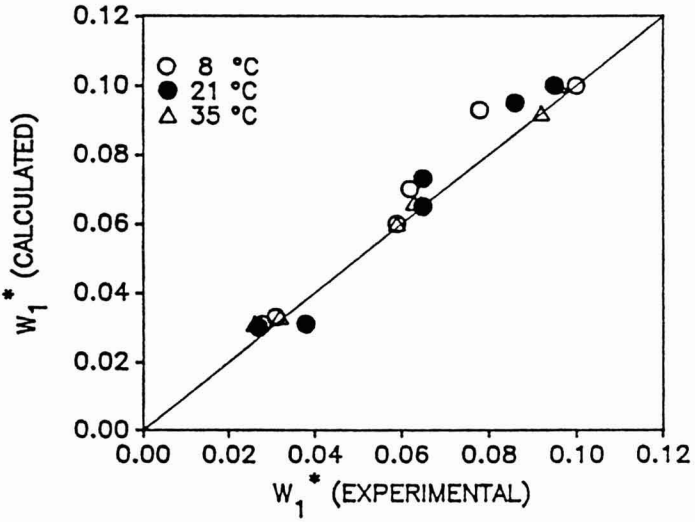

FIG. 1. VERIFICATION OF THE ASSUMPTION THAT NaCl ACTIVITIES IN POTATO TISSUE AND EXTERNAL SOLUTION ARE EQUAL
w_1^*: equilibrium mass fraction of NaCl in potato.

Using the data of Table 1, the cofficients of Eq. (2) were estimated using the multiple regression capabilities of SAS (1985). Initially, the coefficients B_0, B_1 and B_2 that constitute A_0 portion of the model [Eq. (2)] were estimated from the data on "blank" fresh) potato and the potato soaked in pure water by dropping the A_1 and higher order terms in Eq. (2). Then, the coefficients for the A_1 and A_2 portions of the model were estimated by incorporating the numerical values of B_0, B_1 and B_2 in Eq (2) and using the remaining data of Table 1. Estimated values of the regression coefficients (5% level of significance) and their respective R^2 values are listed in Table 2.

TABLE 2
PARAMETERS FOR POTATO IN EQUILIBRIUM WITH NACL-WATER SOLUTION (EQ. 2)

Parameter(*)	Estimated value	R^2
B_0	0.8177	0.98
B_2	0.00017	
C_0	12.4395	0.85
C_1	-0.0789	
D_0	-78.4615	

(*) 5% level of statistical significance.

The statistically significant coefficients (Table 2) were B_0, B_2, C_0, C_1 and D_0. Incorporation of the remaining coefficients in a stepwise regression of the model did not improve the fitting. Substituting for B_0, B_2, C_0, C_1 and D_0, and dropping the remaining terms in Eq. (2),

$$w_3^* = (0.8177 + 0.17\times10^{-3}t^2 + 12.4395w_{1B} - 0.0789tw_{1B} - 78.4615w_{1B}^2)\, w_3^F \quad (3)$$

It should be mentioned that Eq. (3) is purely an empirical relationship and can only be applied to potato/NaCl system.

In the case of an unknown situation where only the composition and temperature of the external solution and w_3^F of fresh potato are known, w_3^* of diced potato is calculated from Eq. (3), and w_1^* and w_2^* are calculated from Eq. (1).

Knowing w_1^*, w_2^* and w_3^*, the equilibrium density of potato, ρ^*, is calculated on a volume additive basis using Eq. (4).

$$w_1^*\bar{v}_1 + w_2^*\bar{v}_2 + w_3^*\bar{v}_3 = 1/\rho^* \tag{4}$$

In Eq. (4), $\bar{v}_1$, $\bar{v}_2$ and $\bar{v}_3$ are the partial specific volumes of NaCl, water and total solid nonsalt, respectively. The correlations for $\bar{v}_1$ and $\bar{v}_2$, and a numerical value for v_3 are available in Biswal and Le Maguer (1989).

Applicability of the model was verified by calculating, the equilibrium densities of potato, ρ^*_{PRED}, for all experimental conditions used in the study. Plotting ρ^*_{PRED} against the experimentally measured equilibrium densities of potato, ρ^*_{EXP}, (Fig. 2), close agreement between the experimental and predicted equilibrium densities is demonstrated.

A point that needs to be addressed is the use of constant $\bar{v}_3$ in the volume additive relation [Eq. (4)]. This assumption implies that the relative shrinkage of potato tissue, from treatment to treatment, was negligible. The appropriateness of this assumption for products with higher moisture and more porous structure, however, needs to be verified.

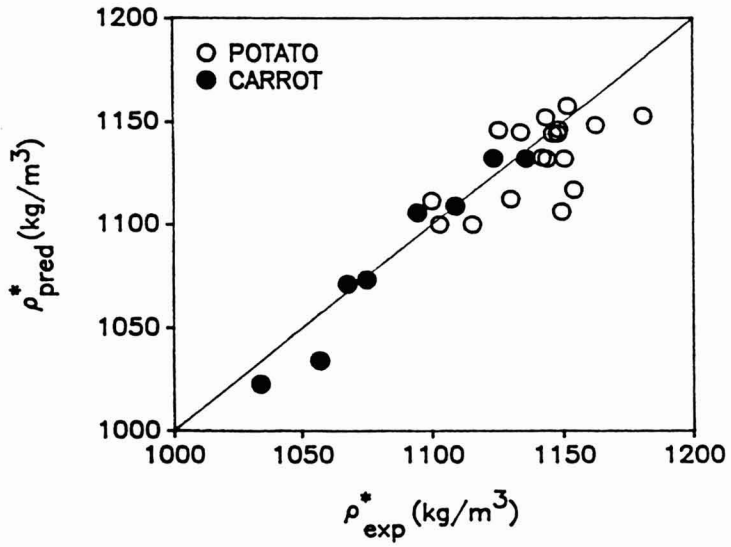

FIG. 2. COMPARISON OF PREDICTED AND EXPERIMENTAL DENSITIES OF POTATO IN EQUILIBRIUM WITH NaCl-WATER SOLUTIONS
Carrot data from Biswal and Le Maguer 1989.

CONCLUSIONS

Equilibrium mass fractions of NaCl and water in potatoes equilibrated with aqueous NaCl solutions can be effectively modelled and from the model these values can be correctly predicted from the mass fraction of total solids in the fresh material at full turgor, the temperature of the treatment, and the NaCl fraction of the original soaking solution.

SYMBOLS

m_o Mass of potato at time zero, kg
m_θ Mass of potato at time theta, kg
t Temperature, °C
$\bar{v}_i$ Partial specific volume of component i, m^3/kg
w_i Mass fraction of component i, kg i/kg total
ρ Density of potato, kg/m^3

Subscripts:

1,2,3 Components 1, 2, and 3
B Bath (external solution)
EXP Experimental
i Components 1, 2, or 3
PRED Predicted

Superscripts:

F Fresh (Material at full turgor)
* Equilibrium

REFERENCES

AOAC. 1984. *Official Methods of Analysis*, 14th Ed., Assoc. of Official Analytical Chemists, Washington, DC.

BARCENAS, M.E., IBARRA, I, WELTI, J., LOPEZO-MALO, A. and ARGAIZ, A. 1990. Osmotic concentration of potato. Presented at 1990 IFT Annual Meeting, Anaheim, June 16–20.

BISWAL, R.N. and BOZORGMEHR, K. 1989. Intermediate moisture frozen vegetables through osmotic dehydration. In *Technical Innovations in Freezing and Refrigeration of Fruits and Vegetables*, pp. 259–266, International Institute of Refrigeration, Paris, France.

BISWAL, R.N., BOZORGMEHR, K., TOMPKINS, F.D. and LIU, X. 1991. Osmotic concentration of green beans prior to freezing. J. Food Sci. *56*(4), 1008–1012.

BISWAL, R.N. and LE MAGUER, M. 1989. Mass transfer in plant materials in contact with aqueous solutions of ethanol and sodium chloride: Equilibrium data. J. Food Process Eng. *11*, 159–176.

HARTAL, D. 1967. Osmotic Dehydration with Sodium Chloride and Other Agents. PhD. thesis. Univ. of Illinois, Urbana, Illinois.

HAWKES, J. and FLINK, J.M. 1978. Osmotic concentration of fruit slices prior to freeze dehydration. J. Food Proc. Preserv. *2*, 265–284.

KIM, M.H. and TOLEDO, R.T. 1987. Effect of osmotic dehydration and high temperature fluidized bed drying on properties of dehydrated rabbiteye blueberries. J. Food Sci. *52*, 980–984, 989.

LE MAGUER, M. 1988. Osmotic dehydration: Review and future directions. In *Proceedings of the International Symposium on Progress in Food Preservation Processes*, Vol. 1, pp. 283–309, CERIA, Brussels, Belgium.

LENART, A. and FLINK, J.M. 1984a. Osmotic concentration of potato. I. Criteria for the end-point of the osmosis process. J. Food Technol. *19*, 45–63.

LENART, A. and FLINK, J.M. 1984b. Osmotic concentration of potato. II. Spatial distribution of the osmotic effect. J. Food Technol. *19*, 65–89.

PONTING, J.D., WATTERS, G.G., FORREY, R.R., JACKSON, R. and STANLEY, W.L. 1966. Osmotic dehydration of fruits. Food Technol. *20*, 125–128.

SAS Institute Inc. 1985. *SAS User's Guide: Statistics*, Version 5 Ed., Cary, NC.

TORREGGIANI, D., MALTINI, E., BERTOLO, G. and MINGARDO, F. 1988. Frozen intermediate moisture fruits: Studies on techniques and product properties. In *Proceedings of the International Symposium on Progress in Food Preservation Process*, Vol. 2, p. 71. CERIA, Brussels, Belgium.

TOUPIN, C.J. and LE MAGUER, M. 1989. Osmotically induced mass transfer in plant storage tissue: A mathematical model. Part II. J. Food Eng. *10*, 97–121.

TOUPIN, C.J., MARCOTTE, M. and LE MAGUER, M. 1989. Osmotically induced mass transfer in plant storage tissue: A mathematical model. Part I. J. Food Eng. *10*, 13–38.

ELECTRICAL CONDUCTIVITY OF SELECTED JUICES: INFLUENCES OF TEMPERATURE, SOLIDS CONTENT, APPLIED VOLTAGE, AND PARTICLE SIZE[1]

SEVUGAN PALANIAPPAN and SUDHIR K. SASTRY[2]

The Ohio State University
Department of Agricultural Engineering
590 Woody Hayes Drive
Columbus, OH 43210

Accepted for Publication August 12, 1991

ABSTRACT

A device was developed to determine the electrical conductivities of foods under ohmic or conventional heating conditions. Orange and tomato juices (serum and various solids contents) were tested in the device. The electrical conductivity of juices increased with temperature and decreased with solids content. The temperature dependence of conductivity was linear, both under conventional and ohmic heating. Experiments on suspensions of carrot juice solids, and polystyrene spheres in sodium phosphate solution showed an increase in electrical conductivity of the suspension with decreasing particle size.

INTRODUCTION

Ohmic heating is considered to be a promising technique for aseptic processing of foods. This method relies on electrical resistance heating which takes place when alternating current is passed through an electrically conducting food product. Since most foods requiring thermal processing contain ionic constituents such as acids and salts, electric current can be passed through them. The food is internally heated due to its electrical resistance, without involving any heating medium and heat transfer surface. Assuming a purely resistive material, the basic principle which governs heat generation is given by:

$$Q = I^2R \tag{1}$$

Salaries and research support provided by State and Federal Funds appropriated to the Ohio Agricultural Research and Development Center, The Ohio State University. References to commercial products and trade names is made with the understanding that no discrimination and no endorsement by The Ohio State University is implied.

[2] Corresponding author.

Journal of Food Process Engineering **14** (1991) 247-260. *All Rights Reserved.*

where, $R = L/(A\sigma)$ (2)

A number of attempts have been made over the years to use electrical resistance heating in several areas of food processing. One of the earliest and successful applications of electricity in food processing was in milk pasteurization (Getchell 1935). Electric pasteurization of milk was widely accepted as a safe method in five states in the U.S., and as a result, by 1938 there were about 50 milk pasteurizers in the nation serving about 50,000 consumers (Moses 1938). However, this method of pasteurization called "Electropure Process," lost its application due to the high cost of processing (de Alwis and Fryer 1990). In their review paper on resistance heating, de Alwis and Fryer (1990) have included a variety of techniques used in the past for thawing, blanching, pasteurization, sterilization and cooking of foods using electricity.

Using the principle of ohmic heating, a heater was developed by the Electricity Council Research Center (ECRC) at Capenhurst, U.K., and licensed to APV Baker who have developed it into a commercial process in the U.K. (Biss *et al.* 1987). It has been reported that ohmic heating is suitable for viscous products and foods containing particulates.

The heating rates of foods under ohmic heating conditions should be known for proper design of the process to ensure product sterility. Since heat generation in foods depend on electrical conductivity (σ), process design requires accurate determination of σ. Standard methods and commercial conductivity meters are available for electrical conductivity measurement (Anon. 1982), but devices are needed for continuous *in situ* measurement for complex heterogeneous systems under ohmic heating conditions. Electrical conductivities of foods have been found to increase with temperature (Dedek 1946; Biss *et al.* 1987; Halden *et al.* 1990). For purposes of process design, it is important that the relation between electrical conductivity and factors such as temperature, solids content, and particle size be known.

The objectives of this study were (1) to develop a device for electrical conductivity measurement during conventional and ohmic heating, (2) to measure electrical conductivities of selected juices over the process temperature range, and (3) to determine the effect of temperature, solids content, applied voltage, and particle size on electrical conductivity of juices.

MATERIALS AND METHODS

Electrical Conductivity Device

An electrical conductivity device (Fig. 1) was developed using a steel tube with a teflon sleeve within it (for electrical insulation and inertness) to make a cylindrical sample chamber. A thermocuple opening was provided at the center

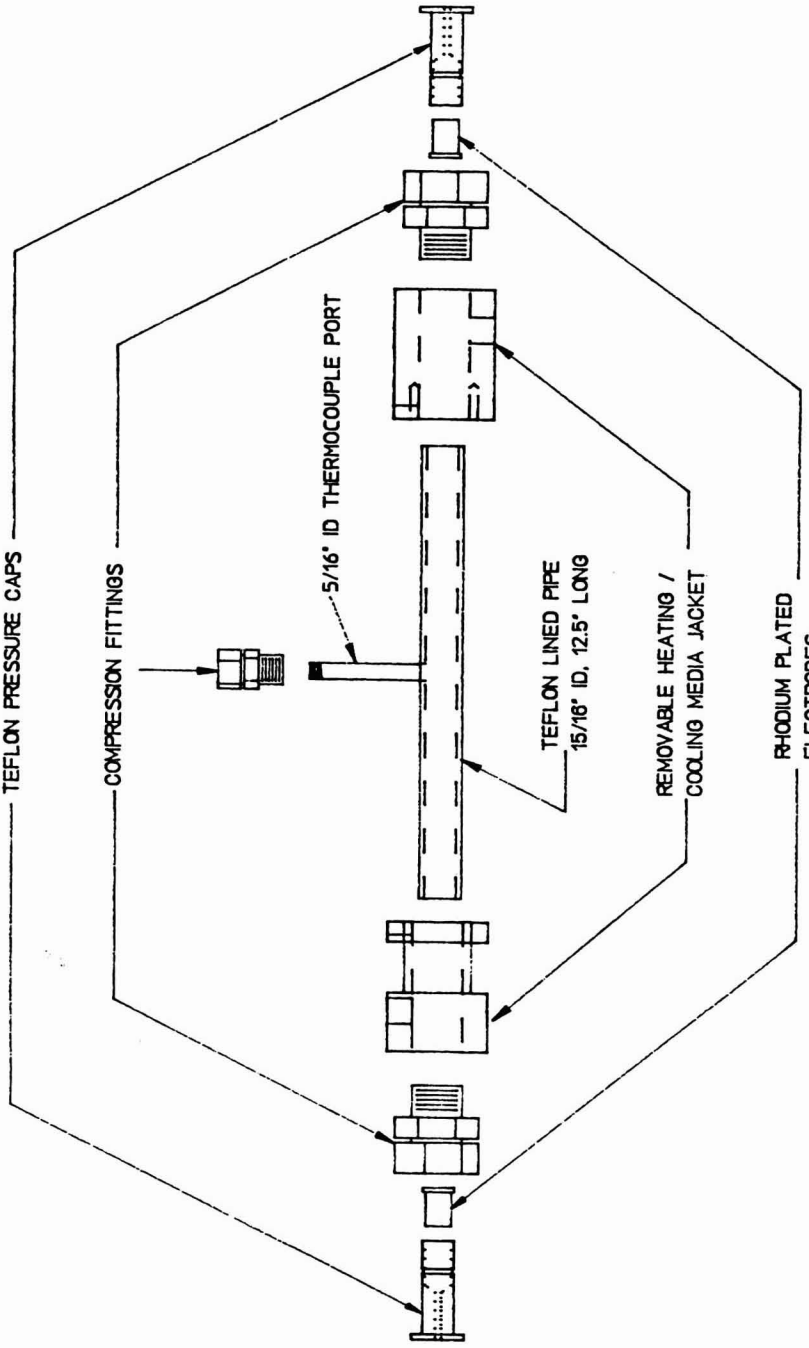

FIG. 1. EXPLODED VIEW OF THE OHMIC HEATING DEVICE

and rhodium plated stainless steel electrodes were secured at both ends by teflon pressure caps. A metallic jacket with a thermocouple opening, and an inlet and an outlet for circulating heat exchange fluids was fitted to the steel tube. The entire unit was attached to a stand in a horizontal position.

The schematic diagram of the experimental set-up is shown in Fig. 2. A T-type copper-constantan, teflon coated thermocouple with a compression fitting was used to measure the temperature at the geometric center of the sample. Voltage

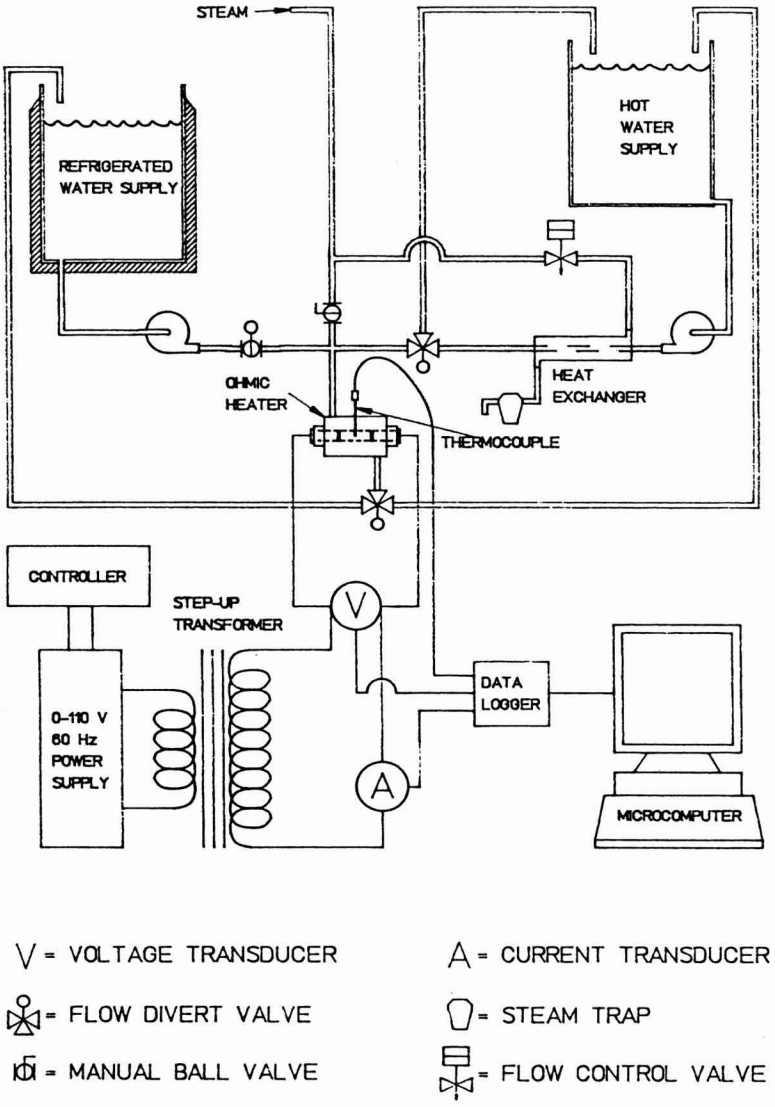

FIG. 2. SCHEMATIC DIAGRAM OF THE EXPERIMENTAL SETUP

and current transducers were used to measure voltage across and current through the samples. A computer control system (Rosemount) was used to maintain constant voltage during heating. A data logger linked to a microcomputer was used to obtain the experimental data at constant time intervals. The accuracy of the conductivity data obtained using this device was tested by determining the electrical conductivities of two salt solutions.

Methodology

Preliminary experiments were conducted using commercial samples of tomato (no salt added) and orange juices. The pH of tomato and orange juices were 4.05 and 3.71, respectively. The samples were poured through the thermocouple port, the thermocouple was inserted, and the system was sealed before ohmically heating to a temperature range of 80–85°C using 140 V a.c. of 60 Hz frequency. The electrode gap was 3.3 cm and the area of cross section of the sample chamber was 4.3 cm^2. Voltage, current, time and temperature data were logged every second during heating. The temperature of each sample was assumed uniform since the difference between the measured values at different locations was within 1.5°C.

The experiments were repeated for varying amounts of insoluble solids in the juices. This was done by resuspending a known amount of previously separated (by centrifugation) solids to the juice serum. Visual observation showed no significant settling of juice solids for a period of less than 30 min, indicating that suspensions did not change significantly during the duration of the experiment. Experiments were also conducted for several power supply voltages, with an electrode gap of 1 cm. The electrical conductivities of tomato and orange juices during conventional heating (using hot water) were also determined by providing low voltage pulses (4–6 V) to the sample at constant time intervals.

Another set of experiments was conducted to determine the effect of particle size on electrical conductivity of juices. Samples used for this study were prepared using carrot juice solids (20%) in 0.1 M sodium phosphate buffer solution. The electrical conductivity of carrots and the phosphate solution at 25°C were measured as 0.035 S/m and 0.68 S/m, respectively. Samples with different mean particle sizes were obtained by subjecting the solids to various periods of time in a blender. The particle size distribution was measured using a Malvern laser particle size analyzer with an attached sample presentation unit for emulsions. The average particle sizes of carrot solids were 560, 505, 484, 453, and 405 μm.

Analysis

Electrical conductivities of samples were calculated from voltage and current data, using the following equations:

$$\sigma = 1/R\ (L/A) \tag{3}$$

or

$$\sigma = (I/V)\ K_c \tag{4}$$

Electrical conductivity was plotted against the corresponding temperature to obtain electrical conductivity curves. The electrical conductivities of the juices were modeled as a linear function of temperature and solids content. The electrical conductivity of juice serum at 25°C was considered as a reference value for modeling. The general form of the equation fitted was:

$$\sigma_T = \sigma_{j25}\ [1+K_1(T-25)] - K_2S \tag{5}$$

$$q'' = \rho C_p(dT/dt) \tag{6}$$

or $$V^2/(Rv) = \rho C_p(dT/dt) \tag{7}$$

i.e., $$(dT/dt) = (V^2\sigma)/(K_c m C_p) \tag{8}$$

Heating rates can be calculated assuming uniform heat generation throughout the sample and negligible heat loss to the surroundings.

RESULTS AND DISCUSSION

Table 1 shows a comparison of electrical conductivities for salt solutions measured in our device, and values either from the literature (CRC 1972), or measured using a commercial conductivity meter. Most of the measured values were

TABLE 1.
COMPARISON OF REFERENCE (σ_{ref}) AND MEASURED (σ_m)
ELECTRICAL CONDUCTIVITY VALUES AT 25°C

Solution	Concentration, M	σ_{ref}, S/m	σ_m, S/m	Difference, %
Sodium Chloride*	0.02	0.20	0.19	5.0
	0.05	0.57	0.55	3.5
	0.17	1.76	1.79	1.7
Sod. Phosphate**	0.03	0.19	0.19	0.0
	0.05	0.34	0.36	5.5
	0.10	0.63	0.67	6.3

* Reference values are literature values (CRC, 1972)
** Reference values are conductivity meter values.

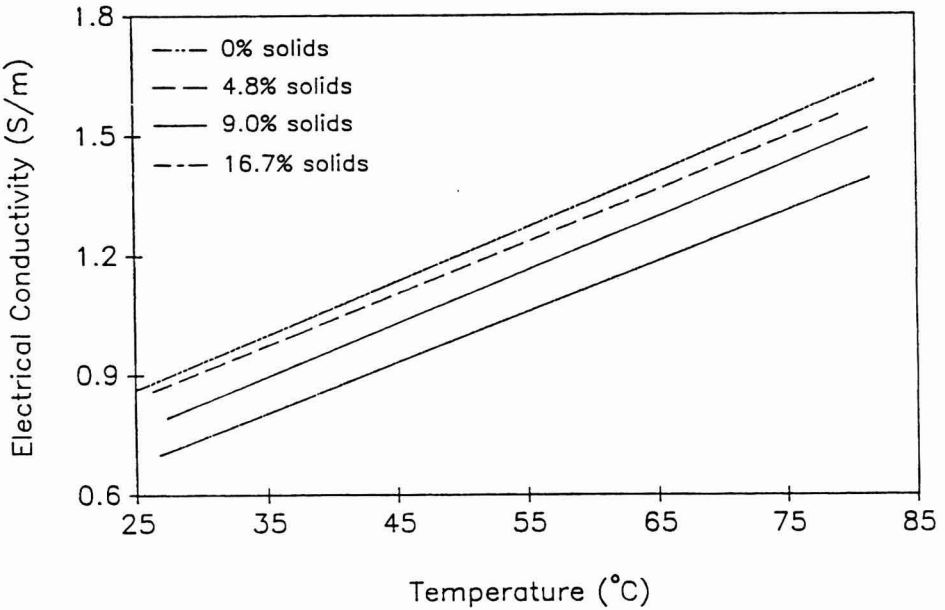

FIG. 3. ELECTRICAL CONDUCTIVITY CURVES OF TOMATO JUICE FOR VARIOUS AMOUNT OF SOLIDS CONTENT

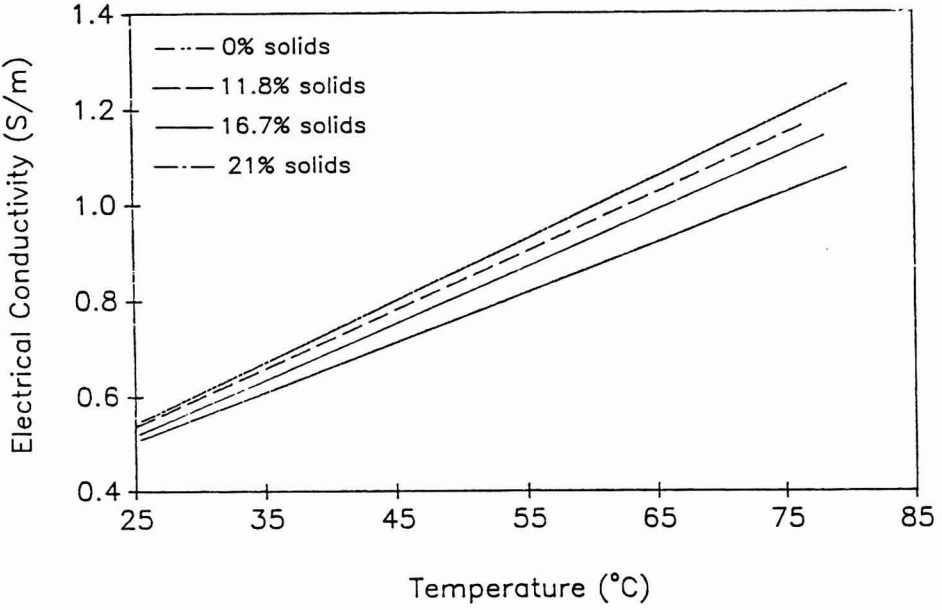

FIG. 4. ELECTRICAL CONDUCTIVITY CURVES OF ORANGE JUICE FOR VARIOUS AMOUNT OF SOLIDS CONTENT

within 5% of the reference values, and the maximum difference determined was 6.3%, indicating satisfactory accuracy for our device.

Electrical conductivity of tomato and orange juices for various amounts of solids content are shown in Fig. 3 and 4, respectively. The conductivities of juices increased linearly with temperature and decreased with solids content. The conductivities of tomato juice with and without solids were higher than those of orange juice at any given temperature. Since the tomato juice had no salt, and its pH was higher (4.03) than that of orange juice (3.71), the results may indicate that the conductivity of orange juice is suppressed by nonionic constituents such as oil and sugars. The presence of other ionic constituents within tomato juice cannot be ruled out on the basis of these data; however detailed chemical analysis of differences between juice samples is outside the scope of this investigation. For the same amount of solids added, the decrease in σ was greater for tomato than for orange juice. It can also be seen that the conductivity curves for tomato juice samples are almost parallel, whereas changes in solids content changed the slopes of the orange juice curves.

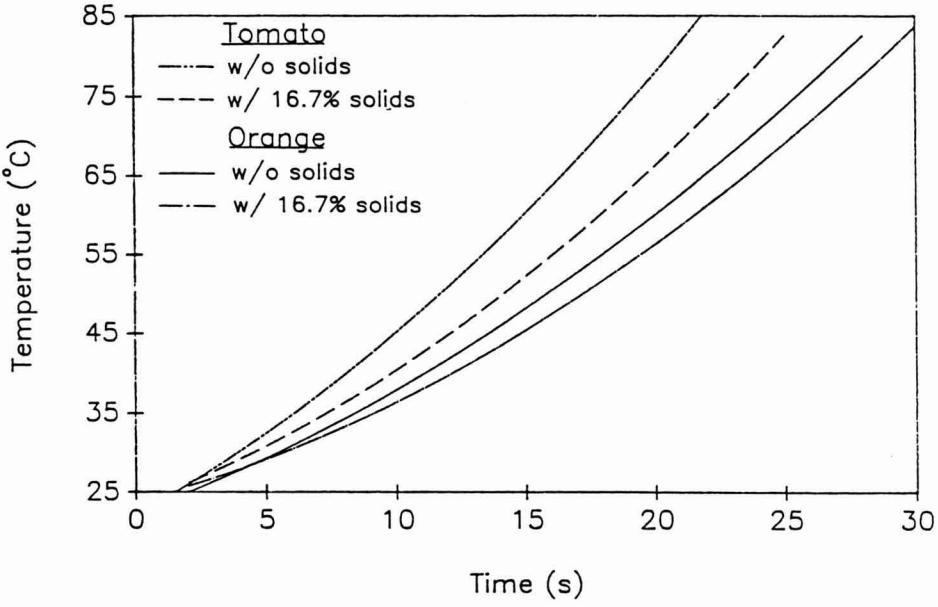

FIG. 5. HEATING CURVES FOR TOMATO AND ORANGE JUICES WITH AND WITHOUT SOLIDS (16.7%) DURING OHMIC HEATING

The heating curves for tomato and orange juices, with and without solids are shown in Fig. 5 These nonlinear heating curves have increasing slopes, since σ increases with temperature. Tomato juice had higher heating rates than orange juice at all temperatures (Fig. 5), which is as expected from the conductivity curves shown in Fig. 3 and 4.

The electrical conductivity of liquids is affected by the nature of ions (chemical composition), ionic movement and viscosity of the liquid, which are all temperature dependent (Anon. 1982). It has been reported that σ of liquids increases with increasing temperatures, opposite to metals but similar to graphite. Increase in electrical conductivity with temperature has been explained (Anon. 1982) by reduced drag for the movement of ions. The drag for ionic movement increases when solids content increases, which may be a reason for the decreasing trend in electrical conductivity with increasing solids content. The drag for ionic mobility may also depend on the size, shape and orientation of particles in the juice solids.

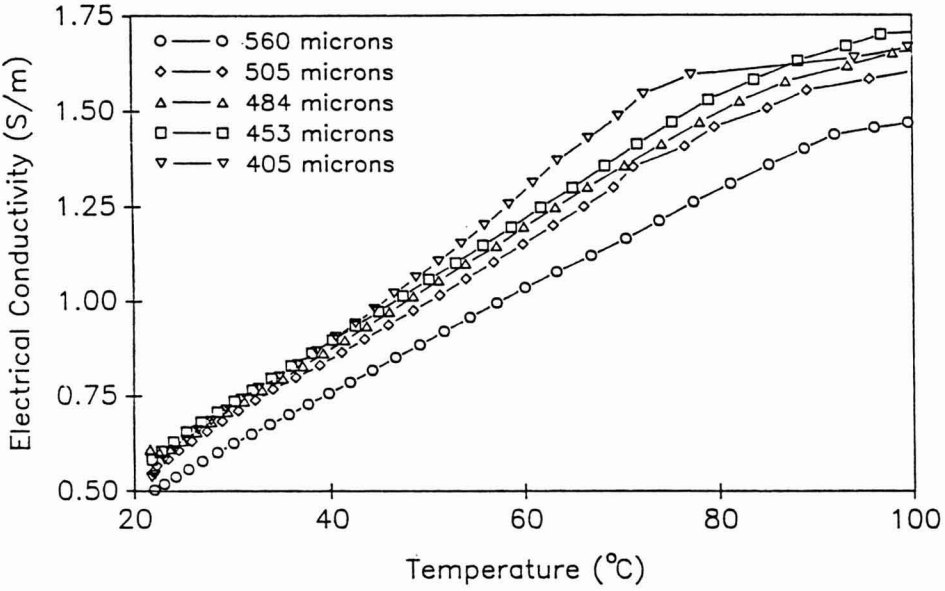

FIG. 6. ELECTRICAL CONDUCTIVITY CURVES FOR CARROT SOLIDS OF VARIOUS PARTICLE SIZES SUSPENDED IN SODIOUM PHOSPHATE SOLUTION

Results of investigations on the role of particle size for carrot juice samples is illustrated in Fig. 6. The conductivity of all samples increased with temperature and decreased with the particle size. Since the solids contents of all samples were the same, the increase in σ with reducing particle size could be due to reduced drag for ionic movement. Another reason considered was the possible release of intracelluar fluids from carrot tissue to the solution which might increase the effective/overall conductivity of the juice. The role of particle size was further investigated by determining electrical conductivities of suspensions of polystyrene spheres (diameters 0.95 and 1.65 cm) in sodium phosphate solution, while maintaining solid volume fraction constant at 0.48. The results of these investigations, as well as those of a mathematical model of Palaniappan and Sastry (1991) showed a slight decrease in electrical conductivity with increasing (non-ionic) particle size. This suggests that the particle size dependence is likely

due to structural rather than chemical effects. Further work is necessary to study other factors such as particle shape and orientation, which affect the electrical conductivity of juices.

The electrical conductivity curves for juices during conventional heating are presented in Fig. 7. The change in σ with respect to temperature is fully linear and the data are in the range of values obtained under ohmic heating conditions.

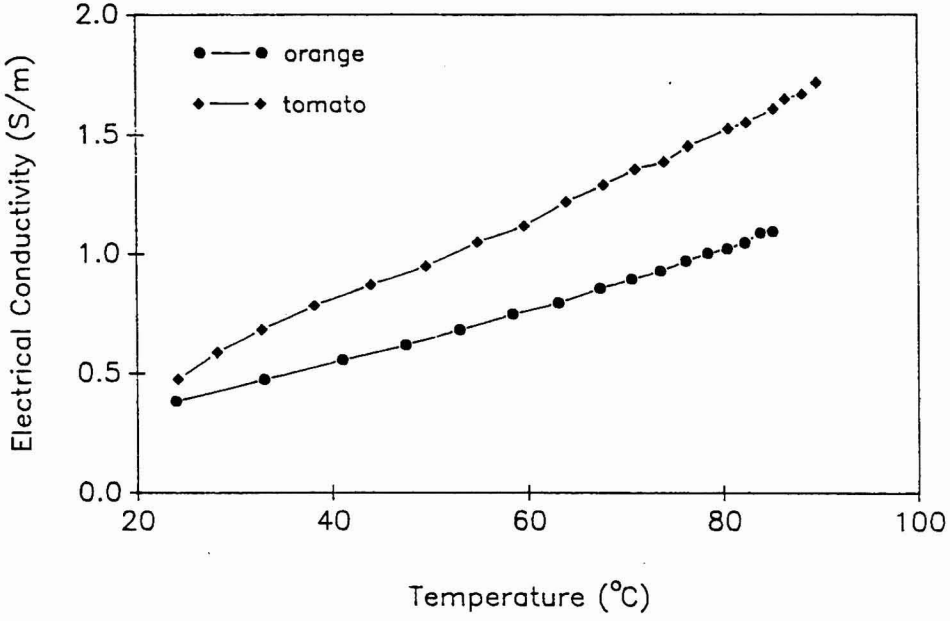

FIG. 7. ELECTRICAL CONDUCTIVITY CURVES FOR TOMATO AND ORANGE JUICES DURING CONVENTIONAL HEATING USING HOT WATER

Table 2 shows the conductivity of juice serum at 25°C (σ_{j25}), temperature constant (K_1), solids content constant (K_2) and the coefficient of determination (r^2) of linear electrical conductivity models for both juices under ohmic heating conditions. Tomato juice had higher values of σ_{j25} and K_2, whereas orange juice had

TABLE 2.
PARAMETERS OF THE ELECTRICAL CONDUCTIVITY MODEL OF EQ. (5)

Juice	σ_{j25} (S/m)	K_1 $(°C)^{-1}$	K_2 (S/m % solids)	r^2
Tomato	0.863	0.174	0.101	0.978
Orange	0.567	0.242	0.036	0.984

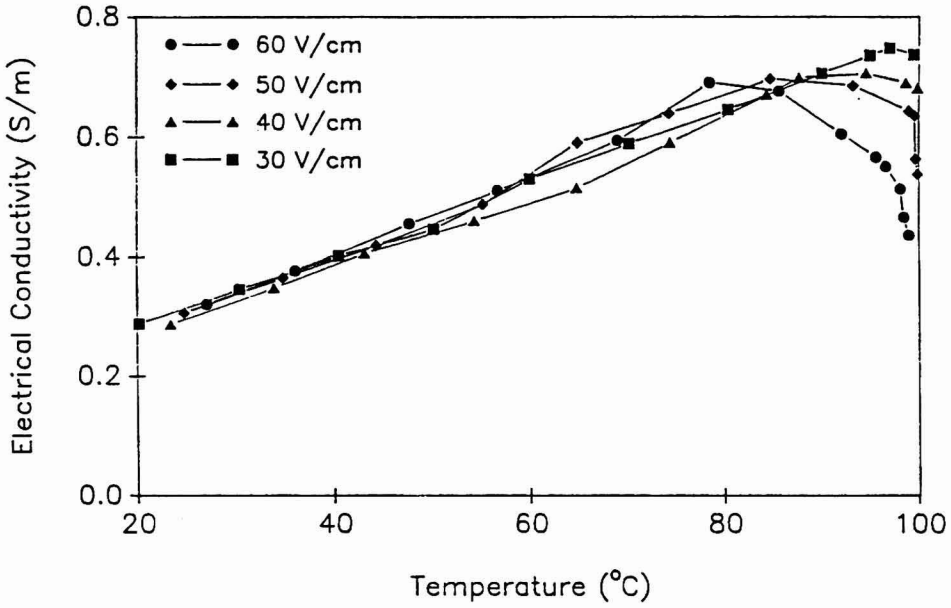

FIG. 8. ELECTRICAL CONDUCTIVITY CURVES FOR ORANGE JUICE SUBJECTED TO SEVERAL VOLTAGE GRADIENTS

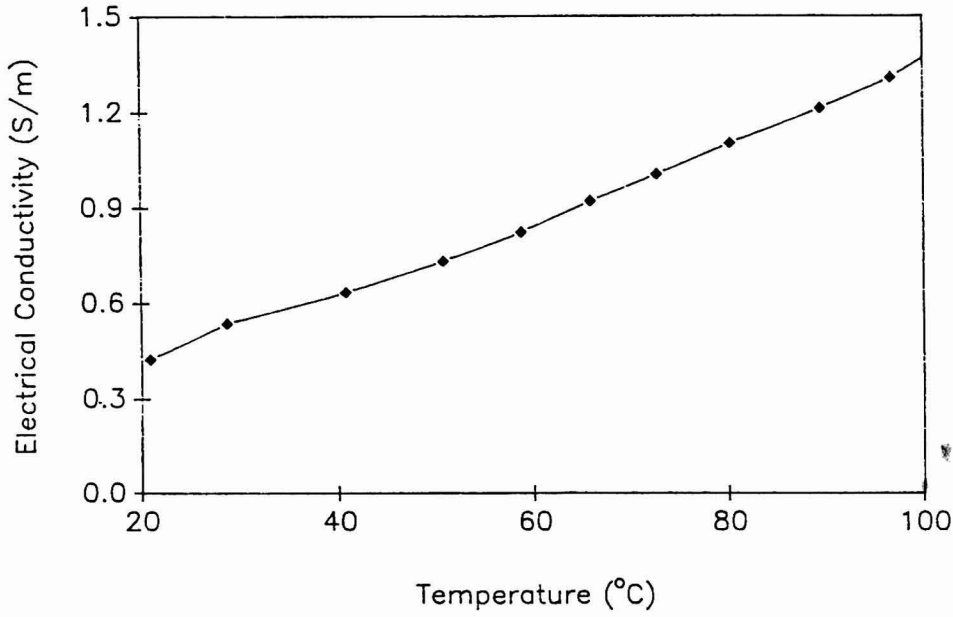

FIG. 9. ELECTRICAL CONDUCTIVITY OF ORANGE JUICE DURING STEAM HEATING

higher value of K_1. The conductivity, particle size, shape and orientation of tomato juice solids may have more effect on reducing σ of juice serum than the orange juice solids.

The data used for regression curves were obtained during heating up to 80–85°C. Above this temperature, the current flow through the sample decreased, due to a sudden decrease in conductivity. Visual observation of samples revealed that this transition was caused by the presence of small gas bubbles near the electrodes. Further studies were conducted to determine whether bubble formation arose from electrolysis or from release of dissolved gases. Repeated heating and cooling of the same sample resulted in little or no change in the behavior. Tests with varying field strengths revealed an increase in transition temperature with decreasing field strengths (Fig. 8). However, under conventional heating (zero field strength) no such transition temperature or gas bubbles were observed (Fig. 9). These observations point to the likelihood of electrolytic gas production in the ohmically heated samples. Notably, both juice samples were acidic, resulting in the potential for electrolytic hydrogen bubble formation.

The decrease in transition temperature with increasing field strength (Fig. 8) indicates the acceleration of gas-producing reactions by increasing electric field strengths. This type of phenomenon has been discussed briefly by Crow (1988) who indicates that for field strengths greater than a few volts/cm, the reaction rate constant for dissociation of weak acids increases with the applied voltage. Thus the hydrogen production rate in a simple weak acid system would depend on the rate balance of the following dependent reactions, both of which would accelerate with increasing field-strength.

$$HA \rightleftharpoons H^+ + A^-$$

$$H^+ + e \rightleftharpoons \frac{1}{2}H_2$$

This may help explain the observed field-strength dependency of the bubble formation temperature. However, while this explanation is useful to gain preliminary insight into electrolytic processes in juices, it must be noted that food systems are inherently complex, and a number of unaccounted factors may be involved in the process. Headspace gas analyses were not performed in these experiments, since they were not part of the objectives.

It is important to note, however, that electrolytic phenomena are highly dependent on the material and condition of the electrode coating used. The present studies did not involve the use of APV electrode material; therefore our results do not imply the occurrence of electrolysis in commercial heaters.

CONCLUSIONS

The electrical conductivity device is useful for measuring conductivities of foods during conventional or ohmic heating. Electrical conductivities of tomato and orange juices increase with temperature and decrease with solids content. The effect of temperature is greater for orange juice, whereas the effect of solids content is greater for tomato juice. Reducing the particle size of juice solids increases the effective conductivity of the juice. Electrolytic gas bubble formation was observed above a field strength-dependent transition temperature; however, these are likely electrode-specific results, and point to the importance of electrode material selection in ohmic heating processes.

NOMENCLATURE

A	Area of cross section of the sample (m^2)
C_P	Specific heat (J/kg°C)
I	Current through the sample (A)
K_C	Cell constant ($K_C = L/A$)
K_1	Temperature compensation constant
K_2	Solids content constant
L	Electrode gap or length of sample (m)
m	Mass of the sample (kg)
Q	Amount of heat liberated (W)
R	Resistance of the sample (ohm)
S	Solids content (%)
T	Temperature (°C)
V	Voltage across the sample (V)
q''	Energy generated per unit volume (W/m^3)
t	Time (s)
v	Volume of the sample (m^3)
ρ	Density (kg/m^3)
σ	Specific electrical conductivity (S/m)
σ_{j25}	Electrical conductivity of juice serum at 25°C (S/m)
σ_m	Measured value of electrical conductivity (S/m)
σ_{ref}	Reference of value of electrical conductivity (S/m)
σ_T	Electrical conductivity at any temperature T (S/m)

REFERENCES

Anon. 1982. Theory and application of electrolytic conductivity measurement, The Foxboro Company, Foxboro, MA (unpublished).

BISS, C.H., COOMBES, S.A. and SKUDDER, P.J. 1987. The development and application of ohmic heating for the continuous heating of particulate foodstuffs. Unpublished document. APV International Ltd., Crawley, West Sussex, U.K.

CRC. 1972. *Handbook of Chemistry and Physics,* 53rd ed, The Chemical Rubber Company, Cleveland, OH.

CROW, D.R. 1988. *Principles and applications of electrochemistry,* 3rd ed., Chapman and Hall, London.

De ALWIS, A.A.P. and FRYER, P.J. 1990. The use of direct resistance heating in the food industry. J. Food Eng. *11,* 3–27.

DEDEK, J. 1946. Lime salts—A measure of the purification of beet juices. Socker *2,* 357–369.

GETCHELL, B.E. 1935. Electric pasteurization of milk. Agr. Eng. *16*(10), 408–410.

HALDEN, K., De ALWIS, A.A.P. and FRYER, P.J. 1990. Changes in the electrical conductivities of foods during ohmic heating. Int. J. Food Sci. Technol. *25,* 9–25.

MOSES, B.D. 1938. Electric pasteurization of milk. Agr. Eng. *19,* 525–526.

PALANIAPPAN, S. and SASTRY, S.K. Modelling of electrical conductivity of liquid-particle mixtures. Food & Bioproducts Proc. (Submitted).

RICE PUFFING IN RELATION TO ITS VARIETAL CHARACTERISTICS AND PROCESSING CONDITIONS

P.R. CHANDRASEKHAR[1]

Instrumentation Engineer
Instrumentation Centre
Veterinary College Campus
Mannuthy, Thrissur-680 651
Kerala

and

P.K. CHATTOPADHYAY

Assistant Professor
Post Harvest Technology Centre
Indian Institute of Technology
Kharagpur, West Bengal-721 302

Accepted for Publication September 23, 1991

ABSTRACT

The effect of rice varietal characteristics, namely, length (L): breadth (B), ratio, amylose and protein contents and processing conditions namely, extent/degree of hydrothermal treatment, degree of milling and percentage of salt addition to rice, on puffing quality were studied in detail. The L:B ratio of varieties tested showed a positive correlation (r = 0.69) with expansion ratio (ER) of puffed rice produced. Total amylose and hot water insoluble amylose contents revealed a definite pattern of relationship, with ER showing predicted peaks at 28.5% total amylose (db) and 13.5% insoluble amylose (db) for highest ER. Protein content showed a negative relationship (r = −0.79) with ER. A new method for determining extent/degree of starch gelatinization, based on Brabender hot paste peak viscosity value (viscosity of 15% slurry retained at 95°C for 20 min.) was used in this study. Normal parboiled and pressure parboiled rice having 425 BU and 240 BU peak viscosities produced highest ER of 7.5 and 9.7, respectively. A 6% milling (minimum) and a 2% salt ($NaCl/CaCl_2$) addition during preconditioning of rice resulted in maximum ER.

[1]Correspondence should be sent to Dr. P.R. Chandrasekhar.

Journal of Food Process Engineering **14** (1991) 261-277.

INTRODUCTION

Puffed rice is popular as breakfast cereal as well as a snack in many countries including India. It is prepared from parboiled (hydrothermally treated) milled rice by high temperature short time (HTST) heating of the dried milled rice in air, oil or sand and also by gun puffing of raw milled rice. After puffing, rice grains expand manyfold to a thoroughly cooked, ready to eat, crisp and porous product.

Apart from proper puffing technique, two important aspects for producing good quality puffed rice are selection of proper paddy varieties and utilization of proper hydrothermal treatment of paddy (rough rice). It is well known to the processors in the cottage industry that all paddy varieties do not expand equally well and hence they invariably choose, by historical evaluation, specific varieties for their trade.

Various research workers (Roberts *et al.* 1951; Antonio and Juliano 1973; Chinnaswamy and Bhattacharya 1983b; Villareal and Juliano 1987) have studied the different varietal characteristics that affected expansion, e.g., total amylose, hot water insoluble amylose, protein content and length, breadth ratio; however, contradictions exist amongst their reported findings which call for further investigation.

Proper hydrothermal treatment in terms of optimum combinations of steaming pressure and time of moist paddy to produce good quality puffed rich have been investigated by Roberts *et al.* (1954) and Chinnaswamy and Bhattacharya (1986), but their findings did not provide quantitative measure of the severity of hydrothermal treatment which would be optimum irrespective of the method adopted.

Few authors have attempted the quantitative assessment of the degree of starch gelatinization in processed foods. Tanaka and Yukami (1969) assessed the degree of gelatinization of starch in precooked rice by incubation with β-amylase followed by estimation of the maltose produced. Birch and Priestly (1973) attempted to quantify the degree of gelatinization in rice based on the amylose/iodine blue value after dispersion in two different concentrations of alkali and related this to a hydrogen bonding effect observed in the infrared absorption spectrum of rice. These methods, however, are relatively slow and complicated. Ferrel and Pence (1964) used amylographs to study the extent of cooking in steamed rice and reported that the reduction in viscosity, when the paste was held in 95°C for 20 min, decreased as steaming or other cooking pretreatment of rice was increased until it reached zero. In the present study, the extent/degree of rice starch gelatinization that took place during parboiling was correlated with Brabender hot-paste peak viscosity values.

It is a common practice for the processors in the rice puffing cottage industry to add common salt solution to the milled parboiled rice and to dry it before

puffing. Optimum milling and addition of salt treatments for obtaining maximum expanded puffed rice were also studied during the present investigation.

MATERIALS AND METHODS

Paddy Varieties

Samples of 12 paddy varieties consisting of short, medium and long types including some traditionally known good puffing varieties were chosen and collected for studying the varietal characteristics (Table 1). They were shade dried to 12–13% moisture content (wb), cleaned and stored in metal containers till further use. However, to study the effect of parboiling, milling and salting on puffing, "Panloi," a commercially used good puffing variety (L = 7.19 mm; B = 2.55 mm; T = 1.71 mm) was used.

TABLE 1.
PHYSICAL DIMENSIONS OF 12 BROWN RICE VARIETIES AND THEIR CLASSIFICATION

Sl. No.	Variety	Length (L) (mm)	Breadth (B) (mm)	L:B ratio	Classification* (ISI)
1	Palmal	6.37	2.34	2.72	Fine
2	Panloi	7.19	2.55	2.82	Fine
3	Kaviraj Sal	7.41	2.17	3.41	Superfine
4	Mugai	6.16	2.28	2.70	Fine
5	Bashkata	7.86	2.37	3.32	Superfine
6	Masuri	5.59	2.16	2.59	Fine
7	Kakhura	6.02	2.70	2.23	Common
8	Patnai	6.91	2.36	2.93	Fine
9	Lata sal	6.63	2.43	2.73	Fine
10	Bhutia (black)	5.99	2.75	2.18	Common
11	Maul	5.65	2.68	2.11	Common
12	Bhutia (white)	5.63	2.62	2.15	Common

* Common = $L/B \leq 2.5$; Fine = $2.5 \leq L/B \leq 3$; Superfine = $L/B \geq 3$.

Physical Dimensions and Classification

The length (L) and breadth (B) of paddy varieties collected were measured using a travelling microscope and were classified according to Indian Standards Institution (I.S.I.) standards as shown in Table 1.

Particle Density and Bulk Density

The particle density (true density) of each sample was determined using an Air Comparison Pycnometer (Model-930, Beckman Instruments, USA) and bulk density was determined using an Ohaus bulk density apparatus (Ohaus Scale Corp., NJ) both measured at 11–12% moisture (wb).

Total Amylose, Water-Insoluble Amylose and Protein Contents

The total amylose content of milled rice was estimated by dispersing rice flour in dilute alkali; neutralizing and measuring the blue color with iodine (Sowbhagya and Bhattacharya 1971). Hot water insoluble amylose of milled rice was estimated by extracting rice flour with hot water, measuring the blue color with iodine, and subtracting resulting soluble amylose value from the total amylose value as determined above. Protein content of milled rice was estimated according to AOAC (1970).

Parboiling and Milling

Paddy samples of 500 g each were soaked in hot water maintained at 70°C to attain approximately 30% moisture content (wb). Each fully soaked paddy sample of 500 g was then subjected to steaming at different steam pressures and time periods, as shown in Table 2, to obtain normal parboiled rice samples with different extents/degrees of starch gelatinization.

TABLE 2.
STEAMING AT DIFFERENT STEAM PRESSURES AND TIME PERIODS TO OBTAIN NORMAL PARBOILED RICE

Sl. No.	Steaming pressure (Kg/Cm^2, gauge)	Steaming time (minutes)
1	0.5	10, 15, 20, 25
2	1.0	5, 10, 15, 20
3	1.5	5, 10, 15, 20
4	2.0	5, 10, 15, 20

In another lot, two 500 g paddy samples were washed with water and then subjected to steam at 2.5 kg/cm^2 gauge pressure for 20 and 30 min, respectively, to obtain pressure parboiled (as traditionally known in India) rice samples.

Each sample was then shade dried to 12–13% moisture content (wb), dehusked in a Satake testing husker (Type - THU) and further milled in a Satake Polisher (Type - TM-05) to approximately 10% by weight bran polish removal for complete removal of bran.

Milling to Different Degrees of Polish

In order to study the effect of degree of milling on quality of puffed rice, samples of different degrees of polish were prepared by milling the brown rice samples for different periods of time. Accordingly, samples at 9 levels of polish (1.64, 2.8, 4.0, 4.5, 5.63, 5.81, 6.85, 8.35 and 10%) were prepared from pressure parboiled paddy samples.

Amylograph Technique

The standard model Brabender amylograph (Brabender OHG, Duisburg) was used to measure the peak viscosities of parboiled rice samples showing their extents/degrees of starch gelatinization.

Rice was ground to pass the 40 mesh screen of the No. 3 Wiley mill. A 15% slurry was prepared by placing 60.0 g ground rice (adjusted to the moisture content) in a Waring blender and approximately 300 g of the required 400 g (adjusted for the actual weight and moisture content of the rice) of distilled water was added. The mixture was slurried 1.5 min and transferred to the amylograph bowl. The remaining water was used to rinse the blender and then transferred to the amylograph bowl. The slurry was initially heated to 30°C. The chart was then adjusted to a zero minute marking and the slurry was heated to 95°C at a rate of 1.5°C per minute. The paste was held at this temperature for 20 min to obtain the peak viscosity value.

Samples were used on the same day of grinding. The Brabender viscograph used was fitted with a 250 cmg sensitivity cartridge and the rpm was kept constant at 75 during the experiments.

Brabender hot paste peak viscosity measurements were carried out for all the 16 rice samples with different extents/degrees of rice starch gelatinization obtained from normal parboiling treatment as well as two rice samples obtained from pressure parboiling treatment. Each measurement was replicated two times.

Salting Treatment

Sodium chloride (NaCl) and calcium chloride ($CaCl_2$) were used as additives (0.5, 1.0, 1.5, 2.0, 2.5, and 3.0% by weight) to study their effects on puffing qual-

ity of rice. Each salt was added to the parboiled milled rice sample in the form of saturated solution and thoroughly mixed before drying to the required moisture content for puffing (10.5–11% wb).

Puffing Technique

Salted and dried samples were puffed in hot air at about 250°C in the continuous heated air fluidized bed puffing machine developed for this purpose (Chandrasekhar and Chattopadhyay 1988).

RESULTS AND DISCUSSION

Paddy Varietal Characteristics in Relation to Puffing Quality

The estimated physical and chemical characteristics of samples of 12 rice varieties (namely, bulk and particle densities, total amylose, hot water insoluble amy-

TABLE 3.
PROPERTIES OF 12 RICE VARIETIES AND THEIR EXPANSION RATIOS AFTER PUFFING

Sl. No.	Variety	Bulk density pb (Kg/m^3)	Particle density pb (Kg/m^3)	Total amylose (%d.b)	Hot water insoluble amylose (% d.b)	Protein (%d.b)	Expansion ratio * (ER)
1	Palmal	831	1467	27.58	11.96	5.43	9.71
2	Panloi	780	1465	28.82	10.35	6.15	9.55
3	Kaviraj Sal	780	1454	26.59	11.16	6.17	9.28
4	Mugai	788	1464	26.92	10.51	5.08	9.12
5	Bashkata	772	1468	31.06	12.74	5.43	8.95
6	Masuri	770	1453	26.92	14.44	6.35	8.81
7	Kakhura	825	1464	31.30	11.31	5.65	7.66
8	Patnai	783	1458	31.22	15.50	5.43	7.41
9	Lata Sal	825	1458	31.55	14.26	6.83	7.41
10	Bhutia(black)	832	1465	26.26	9.75	7.15	7.17
11	Maul	790	1466	31.55	16.78	7.35	5.34
12	Bhutia(white)	812	1451	23.95	9.22	8.40	4.82

* Paddy washed with water and then subjected to steam at $2.5 Kg/Cm^2$ for 30 minutes during hydrothermal treatment.

TABLE 4.
CORRELATION COEFFICIENT BETWEEN DIFFERENT RICE PROPERTIES

Sl. No.	Properties of rice	Correlation with expansion ratio
1	L:B ratio	0.69
2	Bulk density	0.28
3	Particle density	0.27
4	Protein	-0.79

lose and protein contents)and expansion ratios of these samples obtained after puffing are given in Table 3. The correlations obtained, if any, between these properties and expansion ratios are shown in Table 4.

As seen in Table 4, the shape of rice (namely, L:B ratio) was well correlated with the expansion ratio (ER), but bulk density and particle density did not show any signficant correlations. The possible reason for obtaining a comparatively high ER for rice varieties having higher L:B ratio suggested by previous investigators (Chinnaswamy and Bhattacharya 1983b) is that higher amylose contents for longer varieties were responsible for producing higher expansion ratios. This

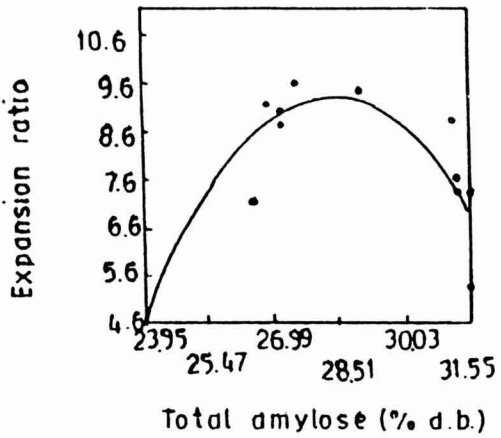

FIG. 1. RELATION BETWEEN TOTAL AMYLOSE CONTENT AND EXPANSION RATIO OF RICE OBTAINED IN THE PRESENT STUDY

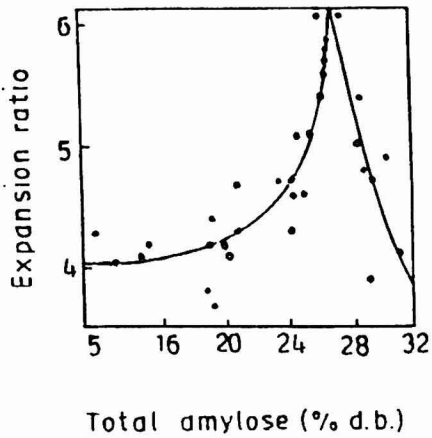

FIG. 2. RELATION BETWEEN TOTAL AMYLOSE CONTENT AND EXPANSION RATIO OF RICE
Reported by Chinnaswamy and Bhattacharya (1983b).

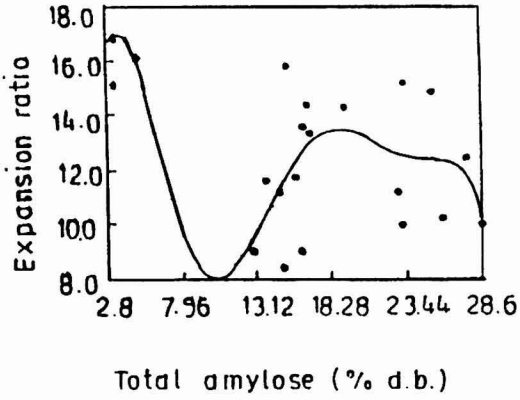

FIG. 3. RELATION BETWEEN TOTAL AMYLOSE CONTENT AND EXPANSION RATIO OF RICE
From data reported by Villareal and Juliano (1987).

could not be collaborated with the present study. Rice varieties chosen in the present study all had high amylose contents and did not show any definite relationship between L:B ratio and total amylose content.

Though the analysis revealed a consistent variation of amylose content with variety, it can be seen from Table 3 that the varieties chosen for the study were all with high amylose content ranging from 23.95–31.55% (db), and almost all of

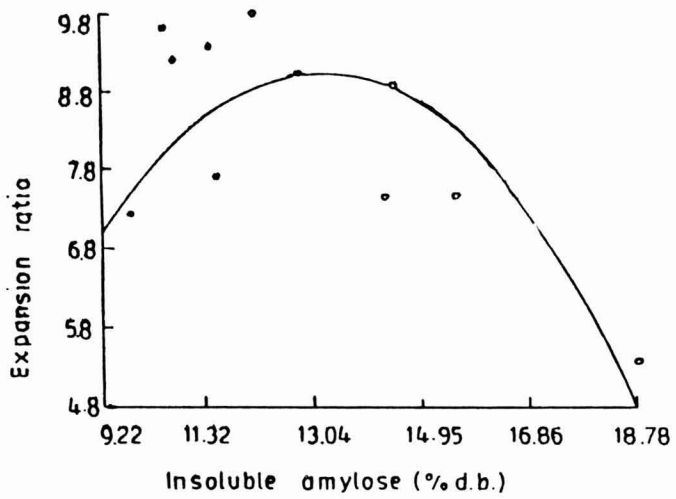

FIG. 4. RELATION BETWEEN HOT WATER INSOLUBLE AMYLOSE CONTENT AND EXPANSION RATIO OF RICE OBTAINED IN THE PRESENT STUDY

them (except two varieties) showed comparatively higher expansion ratios (7–10). When the observed values were fitted to a curve (2nd order, with goodness of fit, $r^2 = 0.77$) as shown in Fig. 1, the predicted optimum total amylose content was found to be about 28.5% (db) for maximum expansion which was similar to the reported data of Chinnaswamy and Bhattacharaya (1983b). The reported data of these investigators, shown in Fig. 2, revealed that among the rice varieties having an amylose content ranging from 5 to 32% (db), comparatively higher expansion ratios were obtained for varieties with higher total amylose content of approximately 24–29% having a peak at 27.5% of total amylose content for highest ER. On the contrary, the data for rice varieties having total amylose content ranging from 2.8–28.6% (db), presented by Villareal and Juliano (1987), showed a negative correlation when fitted to a first order curve. However, a closer observation revealed that when their data were fitted to a smooth curve (6th order, $r^2 = 0.53$), as shown in Fig. 3, a negative relationship with ER existed at lower range of total amylose content, and at higher total amylose range, a similar curve as mentioned above was obtained. Although the third peak was observed at about 28% total amylose content, similar to the present findings, the corresponding expansion ratios were comparatively much lower as compared to the expansion ratios obtained for varieties having lower total amylose content.

Hot water-insoluble amylose contents of rice varieties studied in the present case also showed a definite relationship as shown in Fig. 4 in relation to the ER

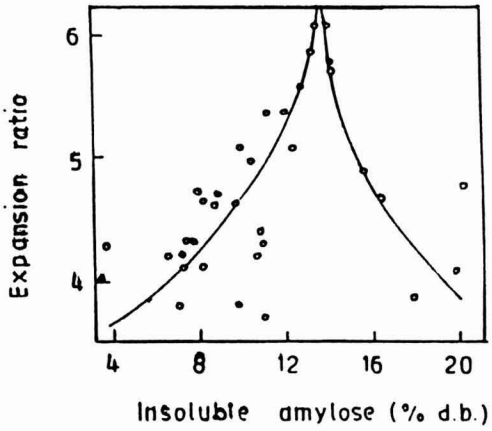

FIG. 5. RELATION BETWEEN HOT WATER INSOLUBLE AMYLOSE CONTENT AND EXPANSION RATIO OF RICE
Reported by Chinnaswamy and Bhattacharya (1983b).

similar to the pattern obtained for total amylose content. This curve (2nd order, r^2 = 0.52) predicted the peak ER for 13.5% (db) hot water-insoluble amylose content. Although in the present investigation, a variety having optimum total amylose content (28.5% db) and optimum hot water-insoluble amylose content (13.5% db) to give maximum expansion was not available, the predicted combination very closely matched with the reported values of Chinnaswamy and Bhattacharya (1983b), as shown in Fig. 6 for comparison. Possibly a further study with isolated starch from waxy and nonwaxy rices may be required to bring forward the exact reason behind this observed phenomenon.

It may be noted that Chinnaswamy and Bhattacharya (1983b) observed comparatively lower ER values for all the rice varieties as compared to the values obtained in the present study. This was presumably due to normal parboiling treatment adopted for their samples (fully soaked paddy was steamed at 1.5 kg/cm^2 gauge for 10 min) giving lower extent/degree of starch gelatinization as compared to the present samples, which were pressure parboiled at 2.5 kg/cm^2 for 30 min giving highter extent/degree of starch gelatinization, as discussed in detail in the following section. It may be further noted that the method of puffing adopted by the above investigators was sand roasting at 250°C, which was similar to the present study where puffing was done with hot air at 250 °C with preconditioned rice. Villareal and Juliano (1987) reported comparatively much higher expansion ratios for all their varieties, which was presumably due to the gun-puffing technique adopted for puffing raw rice with 13–15% moisture con-

tent (wb) and gun chamber pressure of 11.3 kg/cm^2 which was very different as compared to the other two methods.

The correlation analysis further showed a negative relation between protein content and ER ($r = -0.79$) for the rice varieties studied as shown in Fig. 6. Higher protein content in the grain seemed to tend to inhibit the puffed volume expansion and, as the protein content increased, starch content automatically decreased showing the observed effect.

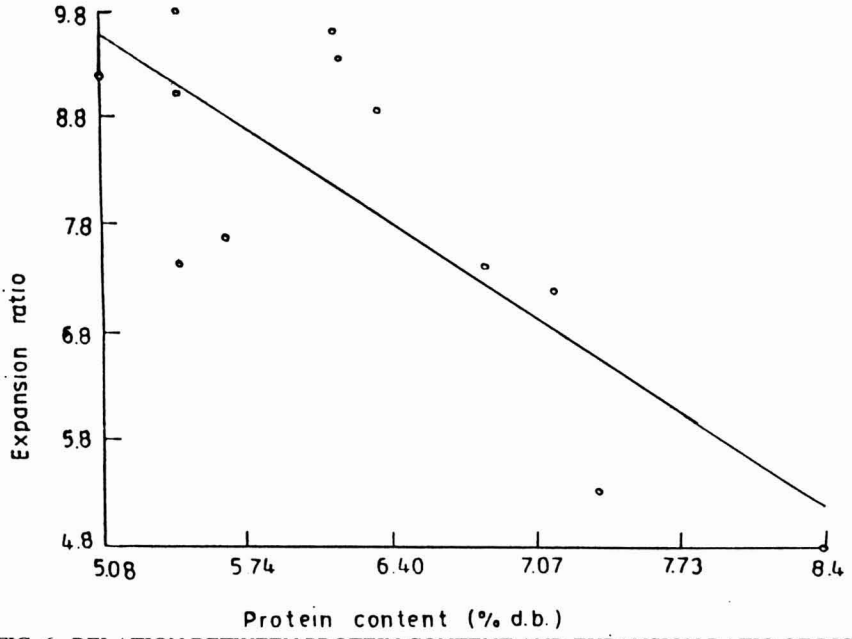

FIG. 6. RELATION BETWEEN PROTEIN CONTENT AND EXPANSION RATIO OF RICE

Quantification of the Extent of Rice Starch Gelatinization in Relation to Puffing

The extent/degree of starch gelatinization as obtained by varying the intensity of hydrothermal treatment with different steaming pressures and periods, was correlated with Brabender hot paste peak viscosity values and their effects on the ER of puffed rice produced were also studied. The data so obtained are given in Table 5.

The variation of Brabender hot paste peak viscosity values of parboiled rice samples with steaming pressures and periods is shown in Fig. 7 confirming the reported data of previous investigators (Ferrel and Pence 1964). For all the steaming pressures studied, the slopes of the peak viscosity curves were higher during the initial period of steaming, and thereafter the curves slowly flattened showing higher initial rate of starch gelatinization. As the steaming pressure increased, higher extent/degree of starch gelatinization resulted within a lesser period of

TABLE 5.
BRABENDER PEAK VISCOSITY VALUES OF PARBOILED RICE SAMPLES AND EXPANSION RATIOS OF CORRESPONDING PUFFED RICE SAMPLES

Treatment No.	Steaming		Brabender viscosity		Expansion ratio of puffed rice
	Pressure (kg/Cm^2 gauge)	Time (minutes)	At 95°C (BU)	Peak Viscosity (BU)	
I Normal Parboiling					
1	0.5	10	960	1390	3.49
2	0.5	15	550	990	4.04
3	0.5	20	310	715	4.76
4	0.5	25	310	705	4.71
5	1.0	5	650	1075	4.85
6	1.0	10	480	890	5.74
7	1.0	15	280	675	5.87
8	1.0	20	260	650	5.37
9	1.5	5	415	740	6.41
10	1.5	10	260	425	7.50
11	1.5	15	260	405	6.35
12	1.5	20	250	390	6.59
13	2.0	5	235	510	6.95
14	2.0	10	235	415	6.27
15	2.0	15	220	380	5.59
16	2.0	20	195	350	5.75
II Pressure parboiling					
17	2.5	20	175	275	9.32
18	2.5	30	170	240	9.70

time. The peak viscosity values obtained for pressure parboiled samples were comparatively lower (Fig. 7). Also, the increasing trend of the Brabender viscosity values after reaching 95°C in all the cases (Table 5) indicates that the intensity of hydrothermal treatment applied in the present study produced samples either completely cooked or overcooked.

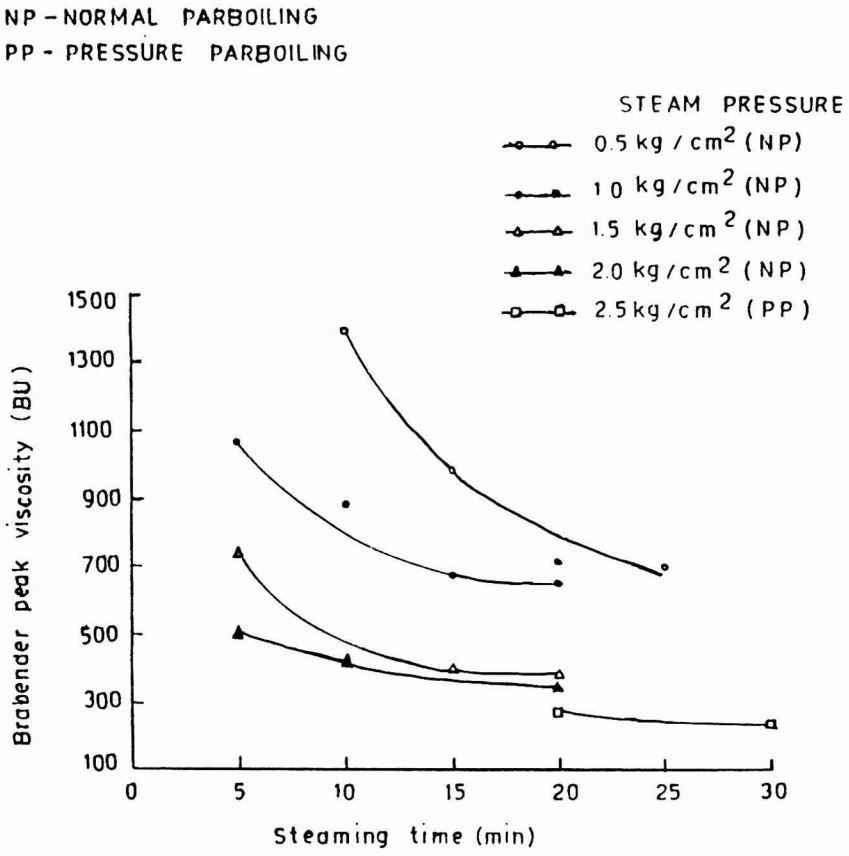

FIG. 7. EFFECT OF STEAMING PRESSURES AND PERIODS ON BRABENDER PEAK VISCOSITY VALUES OF PARBOILED RICE SAMPLES

Data in Table 5 show that for producing maximum expansion of puffed rice, there was an optimum steaming time at each steaming pressure, i.e., 20 min at 0.5 kg/cm^2 with reduction of 5 min in steaming time corresponding to 0.5 kg/cm^2 increase in steaming pressure. However, beyond 2 kg/cm^2 steaming pressure the ER decreased due to excessive grain bursting and, other grain deformation caused during steaming. Normal parboiling at 1.5 kg/cm^2 steaming pressure for 10 min corresponding to peak viscosity of 425 BU produced the highest ER of 7.5 for the puffed rice amongst normal parboiled samples. Pressure parboiled samples at 2.5 kg/cm^2 steaming pressure for 30 min, corresponding to peak vis-

cosity of 240 BU, produced highest ER of 9.7 for the puffed rice.

The variation of ER of puffed rice with Brabender hot paste peak viscosity values is shown in Fig. 8. This experimental data clearly show that the lower the

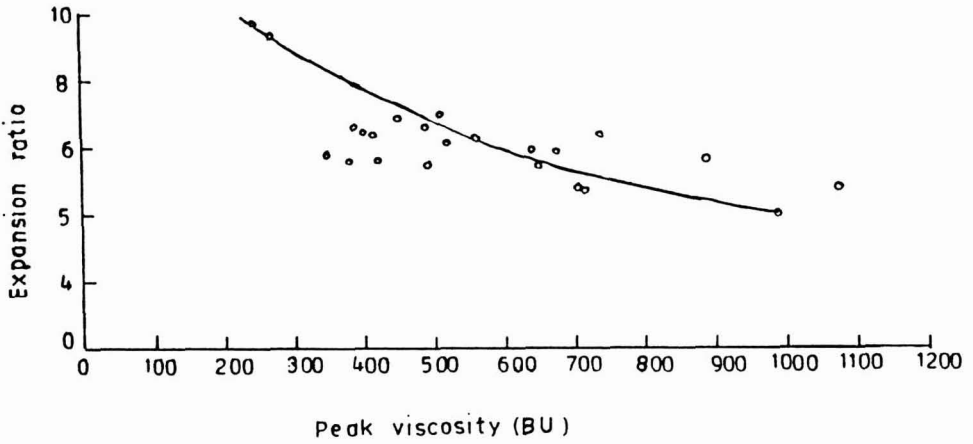

FIG. 8. EFFECT OF BRABENDER PEAK VISCOSITY VALUE ON EXPANSION RATIO OF RICE

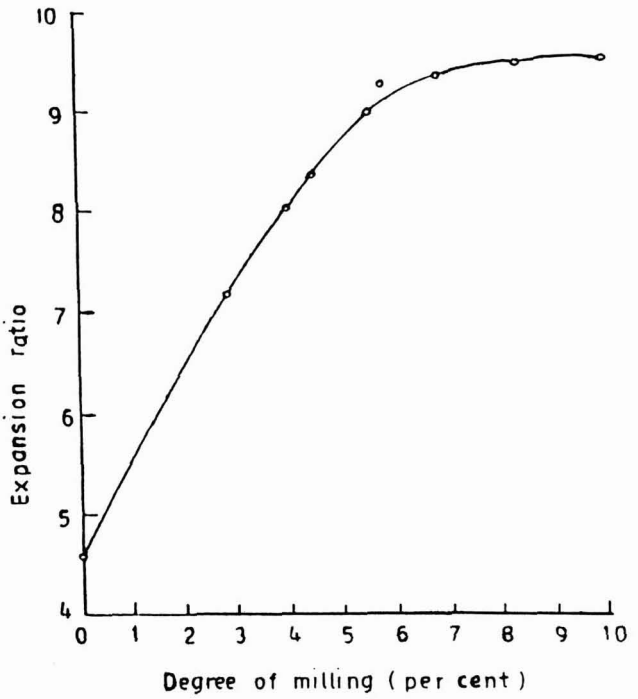

FIG. 9. EFFECT OF DEGREE OF MILLING ON PRESSURE PARBOILED RICE ON ITS EXPANSION

TABLE 6.
EFFECT OF ADDITION OF NaCL AND $CaCL_2$ ON ER OF PUFFED RICE

Salt added	Percentage of salt added (by weight)	ER	Salt added	Percentage of salt added (by weight)	ER
Nil		6.52	Nil		6.52
NaCl	0.5	7.48	$CaCl_2$	0.5	7.37
	1.0	8.22		1.0	8.30
	1.5	8.93		1.5	8.68
	2.0	9.56		2.0	9.48
	2.5	9.53		2.5	9.53
	3.0	9.58		3.0	9.51

peak viscosity value, indicating higher degree of starch gelatinization, the higher the ER of puffed rice obtained. The minimum peak viscosity values obtained for the samples, without any deformation of the rice kernels, by normal parboiling method was 425 BU and by pressure parboiling method was 240 BU. These viscosity values correspond to the highest expansion ratios for the "Panloi" paddy variety cooked under the respective conditions. Beyond these limits the severity of treatment deformed the rice kernels, which resulted in lesser peak viscosity values but lesser expansion of the product. It may also be noted that higher extent/degree of starch gelatinization for the pressure parboiled rice could be achieved without deforming the rice kernels, because of comparatively lesser initial paddy moisture content (about 17%, wb) involved during steaming in the pressure parboiling method.

Optimum Milling and Salting Treatments for Obtaining Maximum Expanded Puffed Rice

The expansion ratios of puffed rice obtained from rice samples having different degrees of milling are shown in Fig. 9. It was observed that a minimum of about 6% degree of milling was necessary to produce optimum expansion for the puffed rice, beyond which the degree of milling showed no appreciable effect on ER. This might be due to the higher resistance offered by the existing bran covering at lower degree of milling against the spontaneous release of high pressure steam formed inside the grain at the time of puffing.

Table 6 shows the increase of ER of puffed rice with the addition of $NaCl/CaCl_2$ at different percentages. The result shows that addition of $NaCl/CaCl_2$ up to 2% by

weight increased the ER by a maximum value of 3 beyond which no significant variation in ER was observed. The above findings confirmed the results of Gerkens and al'Arnaud (1963) who observed that salt helped in increasing the starch expansion by facilitating heat conduction inwards and moisture exit outwards. Two percent salt addition was also found to be optimum during the sensory evaluation of the puffed rice samples. It was also interesting to note that addition of salt produced a smoother surface for the puffed rice, while rice puffed without addition of salt showed uneven blistered surface.

CONCLUSIONS

L:B ratio of all the varieties tested showed a positive correlation with expansion ratio (ER) of puffed rice.

The amylose content and hot water insoluble amylose content of different paddy varieties tested revealed a pattern of relationship with ER showing predicted peaks at 28.5% (db) and 13.5% (db), respectively, for highest ER.

Protein contents of different paddy varieties showed a negative correlation with puffed rice ER.

The extent/degree of starch gelatinization, which was inversely proportional to the Brabender hot paste peak viscosity value, was dependent on the severity of hydrothermal treatment of paddy sample, and showed a definite positive correlation with puffed rice ER.

With hot air puffing, normal parboiled rice sample with 425 BU peak viscosity value produced highest ER of 7.5, whereas traditionally known pressure parboiled rice sample with 240 BU peak viscosity produced highest ER of 9.7 for the same paddy variety tested.

Minimum 6% degree of milling was necessary to produce optimum expansion of the puffed rice kernel.

An optimum of 2% salt addition ($NaCl/CaCl_2$) during preconditioning of rice increased the ER by a maximum value of about 3.

REFERENCES

ANTONIO, A.A. and JULIANO, B.O. 1973. Amylose content and puffed volume of parboiled rice. J.Food Sci. *38*, 915–916.

AOAC. 1970. *Official Methods of Analysis*, Association of Official Analytical Chemists (W. Horowitz, ed.), Washington, DC 20044.

BIRCH, G.G. and PRIESTLEY, R.J. 1973. Degree of gelatinization of cooked rice. Die Stärke *25*, 98–100.

CHANDRASEKHAR, P.R. and CHATTOPADHYAY, P.K. 1988. Continuous rice puffing machine. J. Invention Intelligence *23*(1), 35–36.

CHINNASWAMY, R. and BHATTACHARYA, K.R. 1983a. Studies on expanded rice. Optimum processing conditions. J. Food Sci. *48*, 1604–1608.

CHINNASWAMY, R. and BHATTACHARYA, K.R. 1983b. Studies on expanded rice. Physico-chemical basis of varietal differences. J. Food Sci. *48*, 1600–1603.

CHINNASWAMY, R. and BHATTACHARYA, K.R. 1986. Pressure parboiled rice. A new base for making expanded rice. J. Food Sci. Technol. *23*, 14–19.

FERREL, R.E. and PENCE, J.W. 1964. Use of the amylograph to determine extent of cooking in steamed rice. Cereal Chem. *41*, 1–9.

GERKENS, D.R. and al' ARNAUD. 1963. U.S. Patent 3,076,711. *In Snacks and Fried Products*. Noyes Data Corp., Park Ridge, NJ.

HALL, V.L. and JOHNSON, J.R. 1966. A revised starch-iodine blue test for raw milled rice. Cereal Chem. *43*, 297–302.

ROBERTS, R.L., HOUSTON, D.F. and KESTER, E.B. 1951. Expanded rice product. A new use of parboiled rice. Food Technol. *5*, 361–363.

ROBERTS, R.L., POTTER, A.L., KESTER, E.B. and KENEASTER, K.K. 1954. Effect of processing conditions on the expanded volume colour and soluble starch of parboiled rice. Cereal Chem. *31*, 121–129.

SOWBHAGYA, C.M. and BHATTACHARYA, K.R. 1971. A simplified colorimetric method for determination of amylose content in rice. Starch *23*, 53–56.

TANAKA, M. and YUKAMI, S. 1969. U.S. Patent 3,484,249.

VILLAREAL, C.P. and JULIANO, B.O. 1987. Varietal differences in quality characteristics of puffed rice. Cereal Chem. *64*, 337–342.

CONSEQUENCES OF FOULING AND MACROMOLECULE ADSORPTION ONTO ULTRAFILTRATION MEMBRANE FOR PINEAPPLE JUICE PROCESSING

M.B. DOKO,[1,3] M. VALENTE,[2] M. JACOB[1] AND A. PUECH[1]

[1]*Laboratoire de Pharmacie Galénique,*
Pharmacotechnie et Biopharmacie,
Université de Montpellier I,
Avenue Charles Flahault, 34060 Montpellier Cédex 01-France

[2]*Institut de Recherches sur les Fruits et Agrumes*
IRFA/CIRAD, Domaine St Paul Montfavet, France

Accepted for Publication September 23, 1991

ABSTRACT

Pineapple juice samples were ultrafiltrated using a polysulfone 10,000 molecular weight cut-off (MWCO) membrane. However, to facilitate operations, the ultrafiltration experiments were preceeded by fractionation of juice samples using sequentially Microfiltration/Diafiltration and Ultrafiltration/Diafiltration with 8 μm; 0.4 μm; 0.2 μm and 0.1 μm membranes, using three specific experimental procedures. The 10,000 MWCO membrane was cleansed using a 40°C 1N NaOH solution for a minimum of 30 min, to restore optimal membrane water permeation flux. The effects of selective fractionation processes, pretreatments (using antifoaming agent, hemicellulase, and ammonium sulfate saturation), on permeation rates, concentration levels, protein rejection and protein yields were determined. Water permeation fluxes, measured before and after each UF operation showed a dramatic flux drop from 313 L/hm^2 to 91 L/hm^2 within seven successive 10,000 MWCO membrane experiments. This occurred inspite of suitable membrane washing conditions, pretreatments and selective fractionation processing of samples. The modification, mainly due to fouling, of the integrity of the 10,000 MWCO membrane relative to concentration level was investigated.

INTRODUCTION

Ultrafiltration (UF) applications have been successfully used for fruit juice processing (Yu and Chiang 1986; Rao *et al.* 1986; Thomas *et al.* 1987), and the preparation of protein isolate and concentrate (Olsen 1978; Berot *et al.* 1987;

[3]Correspondence should be sent to Dr. M. B. Doko, Laboratoire de Pharmacie Galénique, Pharmacotechnie et Biopharmacie, Université de Montpellier I, Avenue Charles Flahault, 34060 Montpellier Cédex 01-France.

Journal of Food Process Engineering *14* (1991) 279-289.

Tzeng *et al.* 1988; Deelsie and Cheryan 1988). Besides reducing production costs, these applications have revealed several other advantages, such as improving quality and production yields.

In membrane processing of fruit juices, the main problem in UF is the gradual decrease in flux due to membrane fouling (SHEU *et al.* 1987). Several methods have been tried to prevent this phenomenon, such as increasing shear forces, backflushing, and cleaning (Goldsmith 1971; Watanabe *et al.* 1978; Rudie *et al.* 1984; Chiang and Yu 1987; Rushton and Zhang 1990). The most important UF performance indices are permeation flux, rejection and energy consumption (Chiang and Cheryan 1986; Gathenholm *et al.* 1988; Finnigan 1988; Wu *et al.* 1990). However, less attention has been directed towards the irreversible changes of the membrane behavior, due to foulants.

UF of pineapple juice have been experimented for protein and proteolytic enzyme separation (Doko 1990; Doko *et al.* 1991). Thus, the aim of this study was to determine, using specific membrane processing systems for pineapple juice, the optimal efficiency of UF with regard to membrane integrity (as measured by water flux), volume and protein concentration ratios, and percent protein recovered. The aim was to minimize fouling of the UF membranes.

MATERIALS AND METHODS

Pineapple Juice Preparation

Fresh pineapples, *Ananas comosus* L., Merr., variety smooth cayenne, imported from the Ivory Coast were used in the experiments. Fresh juice extraction was carried out from unskinned, cut fruit using a pilot double-screwed press extractor with a yield of 50% of the fruit mass. The juice was then screen (0.5–1.0 mm) to remove broken shell, blossom cup and to reduce excess pulp (Doko 1990). The resulting juice was then used for membrane processing experiments.

Membrane Processing Equipment

Tubular mineral composite membrane modules (Ceram-Filtres, 34 Lunel-France), with pore size 8 μm, 0.4 μm, 0.2 μm and 0.1 μm with 0.2 m^2 of membrane area each, were used with a pump type LCF4G (PCM—Pompes moineau, Vanves France). The 10,000 molecular weight cut-off (MWCO) Millipore membrane (PTGC 000 05 UF cassette Millipore Corp., Bedford, MA) with a surface area of 0.46 m^2, used in a Millipore HPCF 230 F2 pilot plant, was made of polysulfone with polypropylene as support. Batch process experiments were carried out using specific membrane combinations and treatments as outlined in fractionation procedures shown in Table 1. The permeate was collected separately, while

TABLE 1.
EXPERIMENTAL PROCEEDURES (USING A 10,000 MWCO PTGC MEMBRANE) INVOLVED FOR MEMBRANE PROCESSING OF PINEAPPLE JUICE AFTER SPECIFIC PRETREATMENTS

Experiment	Pineapple juice pretreatments					% DF	VCR	PCR
	pH	Antifoam	Enzyme	Amm. sulfate	MT*			
A	8.5	Yes	No	No	x	47	27	3.3
B	8.5	Yes	No	No	y	43	7	1.7
C	8.5	No	Yes	No	MF**	190	6.3	5.1
D	3.4	No	No	Yes	MF**	190	7.4	7.5
E	3.4	Yes	No	No	MF**	100	30.0	4.0
F	8.5	Yes	Yes	No	MF**	100	26.7	5.0
G	8.5	Yes	Yes	Yes	MF**	100	17.1	8.9

*Membrane pretreatment (MT) were conducted as follow:
x:The pineapple juice was treated using 4 steps, i.e., 8μm; 0.4μm; 0.2μm; and 0.1μm membranes, with percent DF of 58%, 40%, 40%, and 46%, respectively.
y:The pineapple juice was treated using 2 steps, i.e., 8μm; 0.4μm membranes without DF process.

**Membrane pretreatments of pineapple juice were conducted using a single step of membrane processing (i.e., 8μm membrane with 300% DF) before UF PTGC experiments.

Each resulting permeate was processed by the following membrane until the final concentration using the 10,000 MWCO PTGC membrane.

the retentate was returned to the feed tank. Before the first use, the new polysulfone 10,000 MWCO membrane was cleaned with aqueous 0.5N NaOH at 40°C, flushed with water and then rinsed with distilled water as recommended by the manufacturer. Water flux (L/hm^2) was measured after 15 min.

At the completion of each UF experiment the unit was immediately drained, flushed twice with water for 5 min, cleansed, and rinsed with distilled water. Membrane washing and water recycling was continued until the initial water flux was fully restored. Subsequent membrane water fluxes were recorded as soon as inlet and outlet pressures reached 4 and 2 bars, respectively, and the flow rate of permeate and retentate had stabilized. Membrane water flux was measured before and after each experiment to obtain information about the decline in membrane permeability. At the conclusion of the experiment, the membrane, was cleaned and stored in 0.05% sodium azide solution until required for further experiments.

The polysulfone 10,000 MWCO membrane was used successively for UF processing of pineapple juice using different kinds of initial feed solution (Table 1). This series of UF processes was conducted for seven experiments. Water flux, volume concentration ratio (VCR), protein concentration ratio (PCR), protein rejection and yield were recorded at the conclusion of each experiment. Permeate fluxes (L/hm^2) were calculated by dividing the volume of permeate (L) by the surface area (m^2) and the time taken (h) during the corresponding membrane processing. Water flux decline was expressed as the percentage difference in flux before and after each UF experiment. Protein determination (N x 6.25) assays were carried out in feed juice permeate and retentate by the Kjeldhal method. Feed concentrations were expressed as VCR and PCR. VCR is the initial batch volume of the feed divided by the final volume of the retentate and PCR represents the retentate protein content divided by the initial feed protein content. Protein rejection and protein yield were expressed as:

- % Protein rejection = $(1 - C_p/C_r) \times 100$

- % Protein yield in retentate = $(C_rV_r/C_fV_f) \times 100$

- % Protein yield in permeate = $(C_pV_p/C_fV_f) \times 100$

where C_f, C_p and C_r represent protein concentrations in the feed, permeate and retentate, respectively, and V_p, V_f and V_r are the corresponding volumes (Omosaiye and Cheryan 1979; Nichols and Cheryan 1981). This results (under optimal operating conditions, i.e., with overall fractions including retentate and permeate collected) in the solute mass balance equation expressed as:

- $C_fV_f = C_rV_r + C_pV_p + L_m$

where L_m corresponds to solute loss (L) due to adsorption on the membrane (m).

Pretreatments

As the main objective of the operations was rather the separation of proteins and enzymes (i.e., proteolytic enzymes named bromelains) from pineapple juice, different types of pretreatments have been carried out. The pretreatments of the pineapple juice prior to membrane processing included enzyme treatment at pH 8.5 to hydrolyze pectic substances, thus reducing viscosity and improving the filtration rate in membrane processing. Antifoam (12.5 ppm Rhodorsil silicone oil HV 47 350, Rhône Poulenc, France) was used to prevent protein loss and to stabilize the flow rate during membrane processing. The pH of the pineapple juice samples was first raised from 3.4 to 8.5 by the addition of 30% aqueous NaOH solution, after which, the enzyme treatment was conducted at 20°C for 5 h using 200 ppm hemicellulase REG (Gist-brocades Food Ingredients) with moderate stirring.

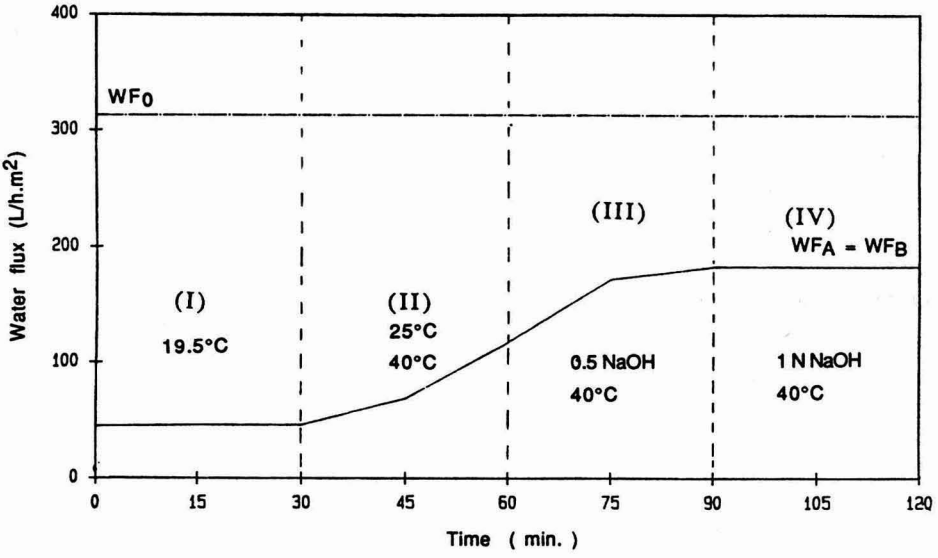

FIG. 1. WATER FLUX RESTORATION OF PTGC MEMBRANE RELATIVE TO CLEANSING CONDITIONS
(I) water at 19.5°C, (II) water at 25°C and 40°C, (III) 0.5N NaOH solution at 40°C; (IV) 1N NaOH solution at 40°C; (—•—) new membrane water permeation flux profile; (— — —) water permeation flux profile recorded from the two first procedures.

$$WF_0 = 313 \text{ L/h m}^2 ; \quad WF_A = WF_B = 183 \text{ L/h m}^2$$

RESULTS AND DISCUSSION

For membrane cleaning efficiency, optimal membrane washing conditions were evaluated using processes A and B (Table 1). The effects of cleaning methods on membrane water flux restoration carried out after these processes are shown in Fig. 1. These demonstrate that a combination of pH and temperature of the cleaning solution, and the washing time is required to restore or to optimize membrane cleansing. Compared to 313 L/hm^2 (= WF_0) water flux of the new 10,000 MWCO cassette, the first experiment, i.e., process A) revealed a significant drop to 183 L/hm^2 (= WF_A), whereas following process B, the resulting water flux (= WF_B) profile indicates none variation, at the end of experiment with a constant 183 L/hm^2. However, this shows that despite good membrane cleaning, which included 1N NaOH solution at 40°C for a minimum of 30 min, restoration of the membrane water flux did not occur in all cases. In addition to the membrane cleaning efficiency, for processing of pineapple juice where insoluble solids and viscous materials are ultrafiltrated, other specific procedures or precautionary measures seem obvious to enhance the processing performance.

Selective fractionation procedures and/or pretreatments significantly influenced membrane performance (Table 2). With regard to UF permeation rates, the sequential fractionation procedures and DF processes removed a major part of

TABLE 2.
UF FRACTIONATION PROCEDURES OF PINEAPPLE JUICE, USING A 10,000 MWCO PTGC MEMBRANE

Experiment	Feed solutions	% DF*	Flux (L/h.m^2)	VCR	% Protein retentate	PCR
Fractionation procedure nr. 1						
A	0.1 µm permeate	47	82	27.0	0.20	3.3
Fractionation procedure nr. 2						
B	0.4 µm permeate	43	32	7.0	0.15	1.7
Fractionation procedure nr. 3						
C	8 µm permeate	190	17	6.3	0.40	5.1
D	8 µm permeate	190	10	7.4	0.75	7.5
E	8 µm permeate	100	25	30.0	0.40	4.0
F	8 µm permeate	100	34	26.7	0.45	5.0
G	8 µm permeate	100	24	17.1	0.80	8.9

*The Diafiltration expressed as % DF = 100 x (volume of water added / volume of feed solution)

Operating conditions: 0.46m2 effective membrane area; T°C maximum = 30 ± 2°C; and the inlet and outlet membrane presures were 4 bar and 2 bar, respectively. The data obtained represent average values of triplicate analysis.

constituents including fibers, pectic substances, sugars, and other suspected solids from the pineapple juice, thus reducing dry matter and viscosity (Doko 1990). As shown for procedure nr. 1 (i.e., Process A in Table 1), this facilitates the UF membrane processing, giving a permeate flux of 82 L/hm^2. This was much higher than those recorded for processes using single steps of 8 μm MF, in spite of high DF processes in both MF and UF operations. Thus, in procedure nr. 3, juice fluxes of 17 L/hm^2 and 25 L/hm^2 were obtained using, respectively, enzyme treatment (process C) and antifoaming agent (process E), whereas the maximum juice flux of only 34 L/hm^2 was obtained with combined pretreatments (using both 12.5 ppm antifoaming agent and 200 ppm hemicellulase for process F). As shown in process D, ammonium sulfate saturation of the feed solution reduced juice flux to 10 L/hm^2, probably by increasing the viscosity of the circulating fluid. However, enzyme treatment of pineapple juice with 200 ppm hemicellulase, plus addition of antifoaming agent prior to significantly increased juice flux to 24 L/hm^2, despite ammonium sulfate saturation for process G.

As far as protein separation efficiency is concerned, the reduction of the fractionation steps to a single 8 μm MF step, provided better conditions for subsequent protein concentration, using the 10,000 MWCO UF membrane. Therefore, in Table 2 the protein content in the resulting retentates ranged from 0.40 to 0.80% by contrast with the low average of 0.20% protein obtained from the first two procedures (i.e., processes A and B). In addition, when combined with UF processing, the ammonium sulfate saturation (known and experimented as a good protein extracting process), resulted in an optimal 0.75% protein at 7.4 fold VCR and 7.5 fold PCR, for, a highest 17.1 fold VCR revealed no further significant improvement as indicated the relatively low 0.80% and 8.9 fold PCR.

As expected, 99% protein rejection (Table 3) showed that virtually no protein permeated the membrane. This, indicating that the separation of proteins having molecular weight (MW) higher than 10,000 daltons was completely controlled by the membrane selective screening, as outlined in procedure nr. 3. Furthermore, 97% of the protein was recovered. So, as concentration level increases simultaneously with the fouling of membrane, the amount of protein loss due to adsorption is strongly influenced at the same time. Therefore, besides ammonium sulfate extraction, and any other pretreatment, the limiting factor for suitable protein separation, i.e., with a membrane fouling reduced as low as possible is the balance between PCR and VCR. A ratio of PCR/VCR $\simeq$ 1 represents the ultimate condition, since reduced fouling is still preferred for ease of UF application.

Thus, despite the fact that the use of ammonium sulfate for protein precipitation reduced the permeation flux by increasing viscosity, maximum protein recovery and the maximum reduction in the amount of protein accumulating on the internal membrane surface were obtained at VCR of 7.4. This can probably be explained by the limitation of chemical interactions between proteins and other

TABLE 3.
UF APPLICATION EFFICIENCY (USING A 10,000 MWCO PTGC MEMBRANE), RELATED TO PARAMETERS INCLUDING PROTEIN SEPARATION (% REJECTION AND RECOVERY) AND THE RESULTING PERCENTAGE OF MEMBRANE WATER FLUX DECLINE, FROM PINEAPPLE JUICE PROCESSING

Experiment	Feed solutions	% Protein rejection	% Protein recovery			PCR/VCR	Water flux decline
			retentate	permeate	loss		
	Fractionation procedure nr. 1						
A	0.1 µm permeate	83	13	71	16	0.12	42
	Fractionation procedure nr. 2						
B	0.4 µm permeate	60	26	77	0	0.24	0
	Fractionation procedure nr. 3						
C	8 µm permeate	97	80	2	18	0.81	29
D	8 µm permeate	99	97	2	1	1.01	0
E	8 µm permeate	98	13	2	83	0.13	10
F	8 µm permeate	98	19	3	78	0.19	0
G	8 µm permeate	99	47	2	51	0.49	22

Operating conditions: 0.46m2 effective membrane area; T°C maximum = 30 + 2°C; and the inlet and outlet membrane presures were 4 bar and 2 bar, respectively. The data obtained represent average values of triplicate analysis.

foulant components, between proteins and membrane, and by the increase of protein-protein aggregations. These lead to low adsorption of macromolecules on the membrane and/or within pores, and to high protein yields. However, at VCR greater than 7.4, despite preventative methods, the increase in membrane fouling and the involvement of proteins in the build up of the adsorbed gel becomes inevitable. As a result, protein losses and the irreversible adsorption of macromolecules on the membrane lead to further membrane spoilage. In addition, it was noticed that even if the action of antifoam relative to flux permeation is effective, at increased VCR, the fouling effects of such an additive, due to its concentration, can prevail with severe negative consequences such as macromolecule adsorption onto the UF membrane, and a resulting decrease of protein recovery.

As concentration increases, the accumulation of macromolecules, such as hemicellulose, proteins and enzymes by the membrane results in the formation of a low water soluble gel matrix on the membrane surface. This gel layer became increasingly compact and tightly attached to the membrane, in spite of DF process. However, the amount of low-MW juice constituents (glucose, fructose and sucrose, citric acid, ascorbic acid, etc.) and minerals are not involved in the formation of the gel, which reduces their proportion in the resulting retentates. Moreover, the effectiveness of the optimal washing conditions for loosening the gel from the membrane was gradually reduced.

The irreversible adsorption of pineapple juice constituents on the membrane

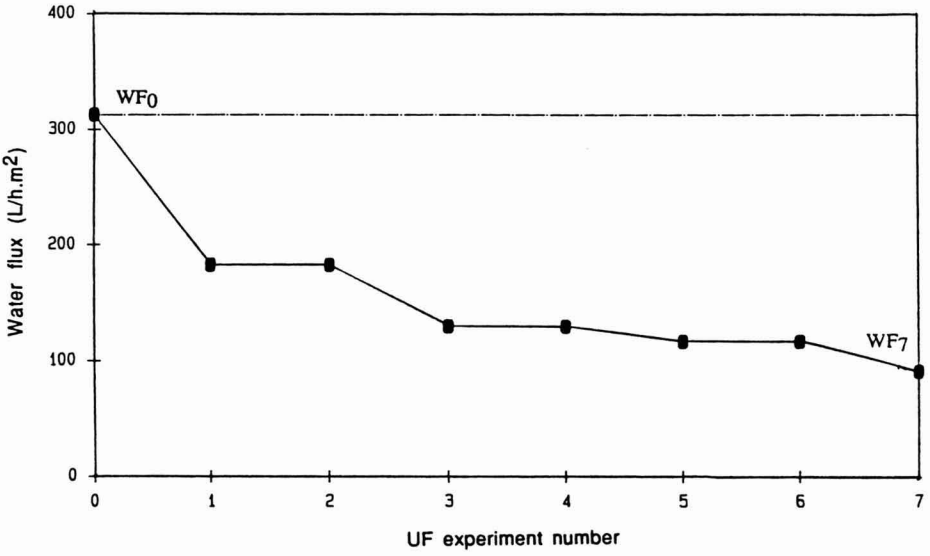

FIG. 2. VARIATION OF THE WATER FLUXES WITHIN SEVEN SUCCESSIVE UF EXPERIMENTS, USING A POLYSULFONE PTGC MEMBRANE FOR PINEAPPLE JUICE PROCESSING.

leads to modification of its structure by reducing membrane pore dimensions. As shown in Fig. 2, this results in an increase in the hydraulic resistance and results in a decline in water flux, as the number of UF experiments increased. Average water flux dropped from 313 L/hm^2 to 91 L/hm^2 (i.e., WF_G), with as shown in Table 2, a 42% decline after the first experiment (process A), even though this procedure had the most fractionation steps.

CONCLUSION

Membrane processing of pineapple juice is a complex process. Macromolecules from such a complex solution resulted in severe plugging of pores and/or in a buildup of a dense sublayer on the surface of the membranes. The efficiency of UF is essentially governed by the foulants. The gel-like layer behaved as a second "dynamic" membrane, which effectively reduces the pore size of the membrane, causing a decline in flux and changing solute rejection. With use, the gel layer deposits become increasingly compact and tightly attached to the membrane, this, in spite of good cleansing conditions. The effectiveness of the optimal washing conditions for loosening the gel from the membrane become gradually inefficient. Since fouling may occur on the membrane surface and/or within the membrane pores, the appropriate pretreatment, such as selective fractionation, and the type of cleaning, and the solute and specially concentration ratios become quite important for optimum filtration of juice and extending the operating lifetime of the membrane.

REFERENCES

BEROT, S., GUEGUEN, J. and BERTHAUD, C. 1987. Ultrafiltration of fababean (*Vicia faba* L.) protein extracts: process and functional properties of the isolates. Lebensm. -Wiss. u.-Technol. *20*, 143–150.

CHIANG, B.H. and CHERYAN, M. 1986. Ultrafiltration of skimmilk in hollow fibers. J. Food Sci. *51*, 340–344.

CHIANG, B.H. and YU, Z.R. 1987. Fouling and lux restoration of ultrafiltration of passion fruit juice. J. Food Sci. *52*, 369.

DEELSIE, W.D. and CHERYAN, M. 1988. Functional properties of soy protein hydrolysates from a continuous ultrafiltration reactor. J. Agric. Food Chem. *36*, 26–31.

DOKO, M.B. 1990. Place de la filtration tangentielle dans les techniques séparatives pour l'optimisation de la production de l'enzyme protéolytique d'Ananas comosus L., Merr. Thesis Doctorat of University of Montpellier I, France.

DOKO, M.B., BASSANI, V., CASADEBAIG, J., CAVAILLES, L. and JACOB, M. 1991. Preparation of proteolytic enzyme extracts from *Ananas comosus* L.

Merr. fruit juice using semi permeable membrane, ammonium sulfate extraction, centrifugation and freeze drying processes. Int. J. Pharm. (in press).

FINNIGAN, T. 1988. Membrane processing. J. Soc. Dairy Technol. *41*, 65–66.

GATHENHOLM, P., PATERSON, S., FANE, A.G. and FELL, C.J.D. 1988. Performance of synthetic membranes during cell harvesting of *E. coli.* Process Biochem. June, 79–81.

GOLDSMITH, C.H. 1971. Macromolecular ultrafiltration with microporous membranes. Ind. Eng. Chem. Fundam. *10*, 113–120.

NICHOLS, D.J. and CHERYAN, M. 1981. Production of soy isolates by ultrafiltration: factors effecting yield and composition. J. Food Sci. *46*, 367-371.

OLSEN, H.S. 1978. Continuous pilot plant production of bean proteins by extraction, centrifugation, ultrafiltration and spray drying. Lebensm.-Wiss. u.-Technol. *11*, 57–64.

OMOSAIYE, O. and CHERYAN, M. 1979. Ultrafiltration of soy water extracts: processing characteristics and yields. J. Food Sci. *44*, 1027–1031.

RAO, MA., ACREE, T.E., COOLEY, H.J. and ENNIS, R.W. 1986. Clarification of apple juice by hollow fiber ultrafiltration: fluxes and retention of odor active-volatiles. J. Food Sci. *52*, 375–377.

RUDDIE, B.J., TORGRIMSON, T.A. and SPATZ, D.D. 1984. Reverse osmosis and fouling studies using ultrafiltration pretreatment. Ann. Meeting of Am. Chem. Soc., Philadelphia, Aug., 124.

RUSHTON, A. and ZHANG, G.S. 1990. Aspects of moving membrane microporus filters, including cleaning. Proceedings, 5th World Filtration Congress, Nice, France (organized by French Filtration Society).

SHEU, M.J., WILEY, R.C. and SHILMME, D.V. 1987. Solute and enzyme recoveries in apple juice clarification using ultrafiltration. J. Food Sci. *52*, 732736.

THOMAS, R.L., GADDIS, J.L., WESTFALL, P.H., TITUS, T.C. and ELLIS, N.D. 1987. Optimisation of apple juice production by single pass metallic membrane ultrafiltration. J. Food Sci. *52*, 1263.

TZENG, Y.M., DIOSADY, L.L. and RUBIN, L.J. 1988. Preparation of rapeseed protein isolate by sodium hexametaphosphate extraction, ultrafiltration, diafiltration and ion-exchange. J. Food Sci. *53*, 1537–1541.

WATANABE, A., KIMURA, S. and KIMURA, S. 1978. Flux restoration of reverse osmosis membranes by intermittent lateral surface flushing for orange juice processing. J. Food Sci. *43*, 985.

WU, M.L., ZALL, R.R. and TZENG, W.C. 1990. Microfiltration and ultrafiltration comparison for apple juice clarification. J. Food Sci. *55*, 1162.

YU, Z.R. and CHIANG, B.H. 1986. Passion fruit juice concentration by ultrafiltration and evaporation. J. Food Sci. *51*, 1501–1505.

RECOVERY AND CONCENTRATION OF FLAVOR COMPOUNDS IN APPLE ESSENCE BY PERVAPORATION

S.Q. ZHANG and T. MATSUURA

Institute for Environmental Chemistry
National Research Council of Canada
Ottawa, Canada, K1A 0R6

Accepted for Publication September 9, 1991

ABSTRACT

Recovery and concentration of flavor compounds from an apple essence (x 500) was attempted by pervaporation using a silicone rubber (polydimethylsiloxane) membrane at room temperature. The flavor components were identified by GC-MS method, and the ratio of concentration of the flavor compound in the permeate to that in the feed was determined for each component. It was found that pervaporation is indeed an effective measure for the above purpose. Concentration ratios above 20 were achieved for flavor components with boiling points lower than 100°C.

INTRODUCTION

Pervaporation is one of the newly emerging membrane separation technologies. Although its history is relatively short, pervaporation has found practical applications in dehydration of alcohols and other organic solvents and in the removal of volatile organic pollutants from water (Brueschke 1989). In pervaporation, while one side of the membrane is in contact with a feed liquid mixture, vacuum is applied on the other side of the membrane to induce permeation of vapors through the membrane. The separation characteristics of the membrane are governed primarily by the nature of the surface of the membrane that is in contact with the feed liquid; membranes are preferentially permeable to water when the surface is hydrophilic whereas they are preferentially permeable to hydrophobic organic compontents of the feed mixture when the surface is hydrophobic. The latter type of pervaporation (membranes with preferential permeability to organic compounds) is currently limited in applications to remove volatile organic compounds

Journal of Food Process Engineering **14** (1991) 291-296.

such as hydrocarbons and halogenated hydocarbons from water (Huang 1991). It is a logical consequence, however, to extend the above application to the concentration of volatile flavor compounds in food liquid, which is obviously an important area of food processing.

The objective of this work is to recover and concentrate by pervaporation some of the important flavor components of apple essence. The flavor components are identified by GC-MS and the concentration ratio of the permeate to the feed solution is obtained for each flavor component. This work is novel in its nature, since the application of pervaporation in the food processing is still scarce in the literature (Bengtsson *et al.* 1989; Voilley *et al.* 1988, 1989).

EXPERIMENTAL

Materials and methods

Natural apple essence (500 ×) supplied by F & C International Co. was used for pervaporation experiments without further treatment. An unbacked silicone (polydimethylsiloxane) membrane of 25.4 μm thickness was generously supplied by General Electric Co.

A static cell with an effective membrane area of 9.6 cm^2 built for reverse osmosis purpose was used for pervaporation experiments with a slight modification. The details of the cell design (Sourirajan and Matsuura 1985) and the pervaporation experiments (Okada and Matsuura 1991) are described in the literature. The flow diagram of the pervaporation system is shown in Fig. 1. Briefly, vacuum was applied on the permeate side of the membrane and the permeate collected in a cold trap for analysis. The pervaporation conditions were: operating temperature, 22°C; downstream pressure, 2.16 mmHg. During 10.2 h of pervaporation period 1.33 g of total permeate was collected in the cold trap. Therefore, the permeation rate was 2.17×10^{-3} g/min. Since the initial feed weight was 25.0 g, the yield of the permeate is 5.32%.

Analysis

A Finningan Model 4010 GC-MS equipped with a 30 m, 0.52 mm I.D. fused silica column coated with a layer of 1.5 μm thickness DBI megabore was employed for the analysis. An interface for the TEKMAR desorber was attached to the column. The interface was used to freeze the sample at −150°C and then rapidly heated to 200°C before the sample was delivered to the chromatography column in order to produce sharper peaks. The helium gas flow rate was 6 mL/min and the oven temperature was programmed to 5°C/min increase in the temperature range −10–150°C. The MS sensitivity was 10^{-7} A/V, ionization current 0.15 mA and electron voltage 50 V. The electron multiplier was set at 1200 V.

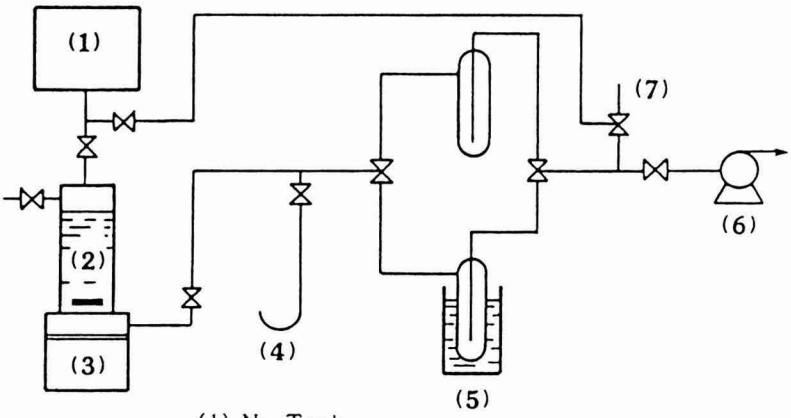

(1) N_2 Tank
(2) Pervaporation Cell
(3) Magnetic Stirrer
(4) Manometer
(5) Cold Trap
(6) Vacuum Pump
(7) Control Valve for Downstream Pressure

FIG. 1. SCHEMATIC FLOW DIAGRAM OF PERVAPORATION EQUIPMENT

A Nova computer system supplied by Data General (Westboro, MA) was attached to GC-MS to identify volatile components in the feed and the permeate samples. Chemical ionization spectra were obtained and compared with standard mass spectra obtained from the National Bureau of Standards (NBS) computerized library (Finnigan 1980). Fifty μL of 5% ethanol solution of 1-phenyl ethanone was added to 1000 μL of the sample as an internal standard. The amount of the chromatography sample injected was 0.3 μL. Then, the column interface was rapidly heated from −150 to 200°C. The air and ethanol peaks were diverted at the outlet of the chromatography column.

RESULTS AND DISCUSSION

The permeate sample of pervaporation experiment consisted of an aqueous solution with a few oily droplets. Apparently, the solubility limit in the aqueous solution was surpassed for some organic components. The amount of the oil phase was negligible compared to the aqueous phase, and, therefore, the analysis was carried out only for the aqueous phase. It should be noted, however, the concentration ratios reported in this paper are conservative values.

TABLE 1.
GC-MS ANALYTICAL RESULTS

		Feed[a]		Permeate[a]	Boiling point,
		Sample 1	Sample 2		°C
1	Acetic acid, Ethyl Ester	0.2		4.5	77.1
2	1-Propanol, 2-Methyl-			6.8	108.0
3	1-Butanol	14.6	15.0	228.5	117.2
4	Propionic acid, Ethyl Ester	0.25	0.25	11.0	99.1
5	Ethane, 1,1-Diethoxy-			53.3	
6	1-Hexene, 4-Methyl-	1.4	0.7	34.0	87.5
7	Propionic Acid	2.3	5.1	2.1	141
8	Propionic Acid, 2-Methyl-, Ethyl Ester	0.2		15.3	109- 111
9	Hexanal	2.3	1.5	33.1	128
10	2-Furfural	2.5	1.4	0.1	161.7
11	Propanoic Acid, 2-Methyl-	5.0	7.2	11.2	153.2
12	2-Hexenal	9.8	9.2	224.7	146-147
13	Butanoic Acid, 3-Methyl-, Ethyl Ester	0.5	0.5	4.0	
14	1-Hexanol	7.4	6.3	91.2	158
15	1,3-Dioxolane, 2-Ethyl-			5.9	
16	1,3-Dioxolane, 2-Propyl-			0.6	
17	3-Heptanol, 3-Methyl-	0.6	0.5	5.3	163
18	Ethanone, 1-Phenyl-	100.0	100.0	100.0	
19	Hexane, 1,1-Diethoxy-			4.7	
20	Hexane,1-(1-Ethoxyethoxy)-			1.2	
21	2-Furfural, 5-(Hydroxymethyl)-	28.4	33.2		114-116

[a] peak area ratio (%) of flavor component to the internal standard (Ethanone,1-Phenyl-).

Both chromatography retention time and mass spectral data were used to identify the solution components. Table 1 shows 20 such components that were identified. Note that number 18 is the internal standard added to the sample. They are four esters, four alcohols, four aldehydes, two acids and six ethers. Compared with components of apple essence found in the literature (Flath *et al.* 1969) the boiling points of components found in this work are significantly higher, indicating that flavor components of lower boiling points were lost during the process of preparing concentrated apple essence that has been used as feed in this work, or they could not be detected by our analytical technique.

The peak area ratio of each component to the internal standard is also given in Table 1. In some cases the component was detected only in the permeate, indicating that pervaporation is a powerful tool for the identification of minute components in the solution by increasing their concentrations to a detectable range. Only in one case [2-furfural, 5-(hydroxymethyl)-] did a relatively large quantity found

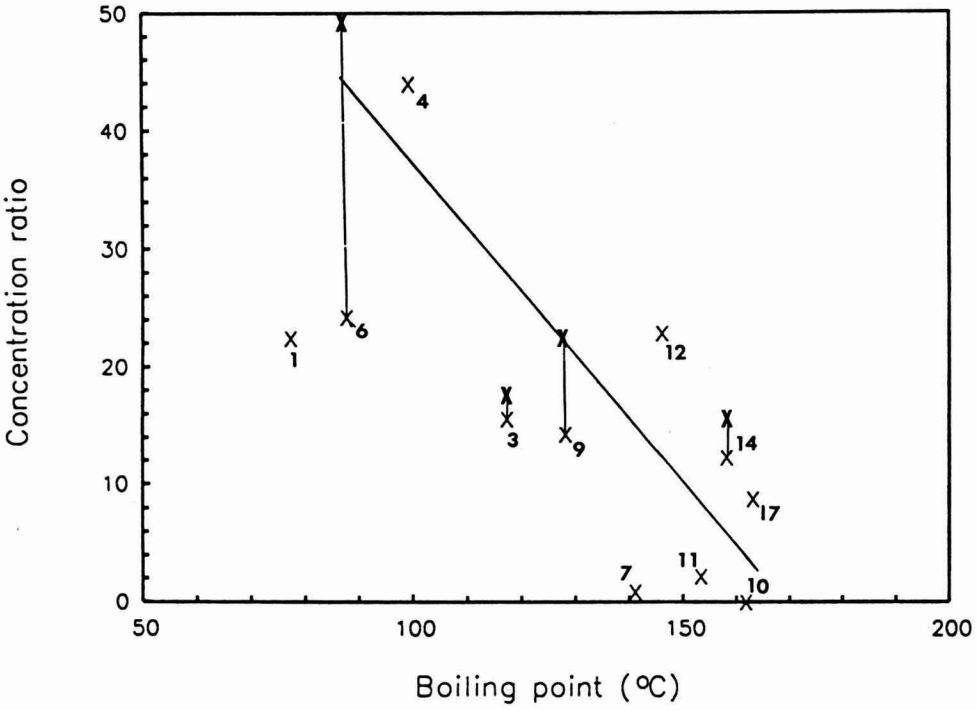

FIG. 2. CONCENTRATION IN THE PERMEATE/CONCENTRATION IN THE FEED VERSUS BOILING POINT OF FLAVOR COMPONENTS

in the feed disappear in the permeate. This is because volatility of this compound was too low. Division of the peak area ratio in the permeate by that in feed allows us to calculate the concentration ratio of the permeate to the feed. The concentration ratio so calculated was plotted versus boiling point in Fig. 2. Eleven flavor compounds for which both concentration ratio and boiling point data are available are included in this figure. The boiling point cover a range from 77 to 163°C. A tendency for concentration ratio to decrease with an increase in boiling point is clearly observed. This is quite natural, since the vapor pressure of the solution component decreases with an increase in the boiling point, resulting in a decrease of the driving force for the membrane transport.

CONCLUSIONS

Pervaporation was proven to be an effective method for the concentration of flavor compounds in the apple essence. The concentration ratio depends on the boiling point of the compound. With respect to the flavor components of relatively low boiling points (100°C) the concentration ratio was above 20.

ACKOWLEDGMENTS

Authors are very grateful to Mr. M.E. Bednas for his assistance to the analysis of flavor compounds, to Ms. R. Rutten for her technical advice and to F & C International Co. for the supply of apple essence.

REFERENCES

BENGTSSON, E., TRÄGÅRDH, G. and HALLSTRÖM, B. 1989. Recovery and concentration of apple juice aroma compounds by pervaporation. J. Food Eng. *10*, 65.

BRUESCHKE, H.E.A. 1989. State-of-art of pervaporation. *In Proceedings of the Fourth International Conference on Pervaporation Processes in the Chemical Industry* (R. Bakish, ed.) pp. 1–12, Bakish Materials Corporation, Englewood, NJ.

FINNIGAN. 1980. NBS Library Compilation, Manual No. 06100-90193.

FLATH, R.A., BLACK, D.R., FORREY, R.R., McDONALD, G.M, MON T.R. and TERANISHI, R. 1969. Volatiles in Gravenstein apple essence identified by GC-Mass spectrometry. J. Chromatogr. Sci. *7*, 508.

HUANG, R.Y.M. 1991. *Pervaporation Membrane Separation Processes,* Elsevier, New York.

OKADA, T. and MATSUURA, T. 1991. A new transport model for pervaporation. J. Membrane Sci. 59, 133.

SOURIRAJAN, S. and MATSUURA, T. 1985. *Reverse Osmosis/Ultrafiltration Process Principles,* National Research Council of Canada, Ottawa, Canada.

VOILLEY, A., LAMAR, T., NGUYEN, T. and SIMATOS, D. 1989. Extraction of aroma compounds by pervaporation technique. *In Proceedings of the Fourth International Conference on Pervaporation Processes in the Chemical Industry* (R. Bakish, ed.) pp. 332–343, Bakish Materials Corporation, Englewood, NJ.

VOILLEY, A., SCHMIDT, B., SIMATOS, D. and BAUDRON, S. 1988. Extraction of aroma compounds by pervaporation technique. *In Proceedings of the Third International Conference on Pervaporation Processes in the Chemical Industry* (R. Bakish, ed.) pp. 429–438, Bakish Materials Corporation, Englewood, NJ.

NONDESTRUCTIVE MEASUREMENT OF TRANSIENT MOISTURE PROFILES AND THE MOISTURE DIFFUSION COEFFICIENT IN A POTATO DURING DRYING AND ABSORPTION BY NMR IMAGING

RONGSHENG RUAN
Department of Agricultural Engineering
University of Illinois
Urbana, IL 61801

SHELLY J. SCHMIDT
Division of Foods and Nutrition
University of Illinois
Urbana, IL 61801

ARTHUR R. SCHMIDT
Department of Civil Engineering
University of Illinois
Urbana, IL 61081

and

J. BRUCE LITCHFIELD[1]
Department of Agricultural Engineering
University of Illinois
Urbana, IL 61801

Accepted for Publication August 27, 1991

ABSTRACT

A nondestructive method to measure the internal moisture distribution and to determine the effective moisture diffusion coefficient for a potato during drying and absorption was developed using NMR imaging and numerical modeling techniques. The coefficients obtained were 1.04 to 7.28 x 10^{-10} m^2/s, for moisture contents between 40% and 55% (wb), during drying with a sample temperature of 40°C; and were 9.78 x 10^{-12} to 2.33 x 10^{-11} m^2/s, for moisture contents between 56% and 60%, during absorption at 23°C.

[1]Correspondent: J. Bruce Litchfield, 360 AESB, 1304 W. Penn. Ave., Urbana, IL 61801.

Journal of Food Process Engineering *14* (1991) 297-313.

INTRODUCTION AND OBJECTIVES

Potatoes are the leading vegetable crop in the world with an annual farm value of nearly $30 billion for more than 340 million tons. Water is one of the most important components affecting the physical properties and quality of potatoes and potato products.

The way water affects the physical nature and properties of potatoes and their products is complicated. The internal moisture distribution and moisture diffusion coefficient are very important parameters for studying the quality and structural changes during storage, handling and processing. Understanding the basic relations governing the transfer of moisture within a potato will lead to better process control.

Tremendous efforts have been directed towards investigating this subject (Callaghan and Eccles 1979; Chu and Hustrulid 1968; Crank and Park 1976; Kashkina 1979; Lomauro and Bakshi 1985; Meyer and Brown 1988; Syrief *et al.*1987). Several methods for determining moisture diffusion coefficients have been developed. Crank and Park (1976) grouped these methods into five different categories: (1) permeation methods, (2) sorption and desorption methods, (3) concentration distance curve methods, (4) radio tracer methods, and (5) nuclear magnetic resonance and self-diffusion methods. Until recently, none of these techniques have used NMR imaging to measure moisture profiles nondestructively for the determination of the diffusion coefficient.

Magnetic resonance imaging (MRI) has become a premier method for producing anatomical images from humans and animals. Recent developments in MRI instrumentation have greatly improved the spatial resolution, and images on a microscopic scale are now possible. Lauterbur (1986) reported microscopic images of a snail and Zhou *et al.* (1989) used three-dimensional projection reconstruction volume imaging to obtain microscopic images of rat spleen. Applications of MRI in the field of medicine have been highly successful, and now innovative, nonmedical applications are being introduced. Blackland and Mansfield (1986) studied diffusion in liquid-solid systems by NMR imaging. The sample was removed from the water before the MRI data was acquired, which made the water absorption a discontinuous process. One-dimensional spin projections were used for the integration of moisture movement. Guillot *et al.* (1989) used NMR imaging to monitor the drying of a porous rock. Rothwell *et al.*. (1984) suggested that MRI may be a powerful new technique for applications in the study of absorption and diffusion processes in polymers, but MRI has had only a few applications in the study of food materials (Bell 1986; Jenner *et al.* 1988; Perez *et al.* 1988; Song and Litchfield 1988; Ruan and Litchfield 1989; Chen *et al.* 1989; McCarthy and Perez 1989; Heil *et al.* 1990; McCarthy 1990; Song *et al.*1990).

The objectives of this study were to: (1) develop a method based on nuclear magnetic resonance imaging for measuring the internal moisture distribution pro-

files of a potato cylinder during drying and absorption and (2) develop a method to estimate the moisture diffusion coefficient in potato based on the moisture content data collected from the NMR images.

THEORY AND METHODS

Fick's law has been applied to some mass transfer problems in food materials. Fick's second law of diffusion written in cylindrical coordinates (r,θ,z) is:

$$\frac{\partial M}{\partial t}=D[\frac{\partial^2 M}{\partial r^2}+\frac{1}{r}\frac{\partial M}{\partial r}+\frac{1}{r^2}\frac{\partial^2 M}{\partial \theta^2}+\frac{\partial^2 M}{\partial z^2}] \quad (1)$$

Where D is the effective moisture diffusion coefficient (m^2/s), M is the moisture content (%, wb), t is time (s), and r is the radius (m). This equation is valid when: (1) the pressure and temperature gradients in the potato are negligible, (2) the moisture gradients are the sole driving force for mass transfer, and (3) the flow of moisture within the potato cylinder occurs by diffusion (liquid and/or vapor). Assuming that mass transfer resistance at the end surfaces of the cylinder is negligible and that moisture transfer is one dimensional in the radial direction, the above equation can be simplified, so that the moisture movement in the central slice of a long potato cylinder during drying and absorption is governed by the following partial differential equation (Welty *et al.* 1984):

$$\frac{\partial M}{\partial t}=D[\frac{1}{r}\frac{\partial(r\frac{\partial M}{\partial r})}{\partial r}] \quad (2)$$

with the initial condition M(0,r), for time t = 0, and radius $0 \le r \le R$, and the boundary condition M(t,R), for r = R and any $t > 0$. Both sets of conditions can be measured by MRI.

Measurement of Moisture Profiles and Prediction of the Diffusion Coefficient

At any time, t_i, the moisture content $M(t_i,r_j)$ at any radius, r_j, can be measured from moisture profile data obtained from NMR proton density images. The moisture content can also be calculated using Eq. (2). The effective diffusion coefficient, D, corresponding to a particular average moisture content of the sample, was determined by iterating different values for D to minimize the error (ERR) between the MRI measured moisture contents (M_m) and the moisture contents predicted (M_p) by Fick's law in the following objective function:

$$ERR=\frac{1}{5}\sum_{j=0}^{4}(M_m(t,r_j)-M_p(t,r_j))^2 \quad (3)$$

The relationship between the diffusion coefficient and moisture content was obtained by determining D for different moisture contents.

Cylindrical potato samples were used. The samples were 20 mm in diameter and 70 mm in length. The ratio of length to diameter of the sample was greater than 3 to help ensure that the moisture transfer in the center of the sample was not influenced by the ends of the sample. In addition, the two end surfaces were coated with wax. The sample was then suspended by a sample holder mounted in the center of an 8.8 cm inside diameter imaging probe (Fig. 1) for drying. In the

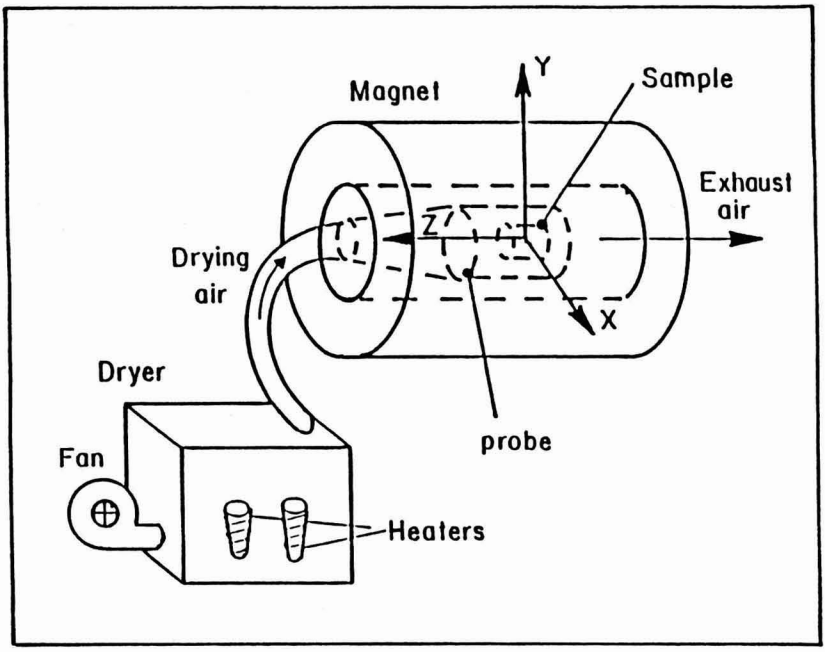

FIG. 1. A SCHEMATIC DIAGRAM OF THE DRYING SYSTEM

absorption experiments, the potato sample was first dried (since the moisture content of the fresh potato is already very high), then the sample was put into a tube full of water for absorption. Both the initial and the transient proton density profiles during drying and absorption were measured using a Spectroscopy Imaging Systems (SIS) 4.7 Tesla NMR imaging system (Fig. 2).

A spin-warp sequence was employed for the acquisition of free induction decay (FID) data. The spin-lattice relaxation time, T_1, was measured using the inversion recovery pulse sequence (Stark and Bradley 1988). The spin-spin relaxation time, T_2, was measured using the Hahn spin-echo sequence (Stark and Bradley 1988). The T_2 values obtained with this technique are apparent T_2 values, which include the magnetic field inhomogeneity, molecular diffusion, and other effects. If the obtained moisture profiles were not accurate enough, measurement

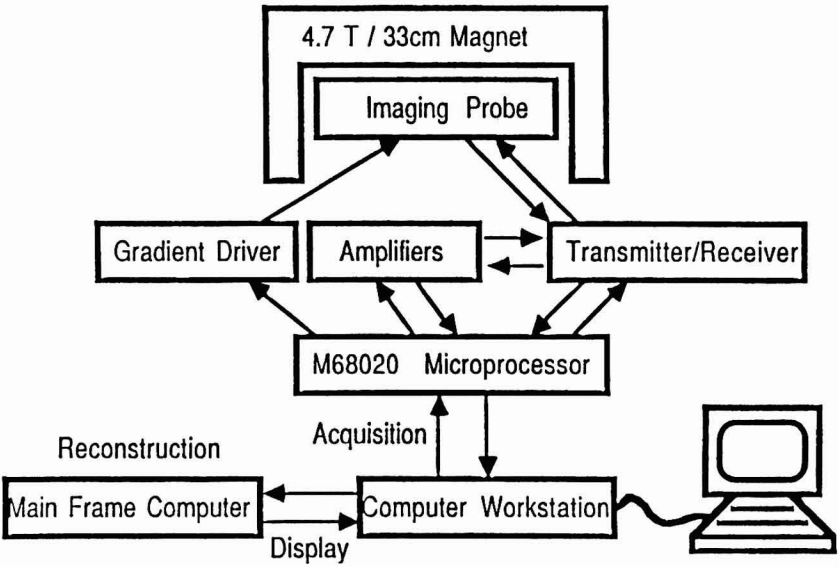

FIG. 2. NMR IMAGING SYSTEM

of the local T_1 and true T_2 values would have been necessary. However, the results of the moisture profiles were accurate to within 3% moisture content, as compared to profiles from vacuum oven measurements, so no localized T_1 and T_2 mappings were obtained. Both T_1 and T_2 were measured as functions of time and average sample temperature during drying as shown in Fig. 3 and 4, respectively. Since the T_1 of the potato ranged between 0.9 and 1.8 s, the interexperiment delay variable, or time of replication, TR, in the MRI system was set to 8 s, which was more than 4 times larger than the greatest T_1 value. The value of TR was selected to decrease the spin-lattice effects. Since T_2 changed with drying time and temperature, as shown in Fig. 3 and 4, each echo time, TE, in the spin-warp sequence was selected to correspond to the appropriate T_2 values. Thus the approximate signal intensity, S, where

$$S = K\rho[1-e^{-\frac{TR}{T_1}}]e^{-\frac{TE}{T_2}} \tag{4}$$

and K is a constant, was only affected by the change in hydrogen nuclei density, ρ.

The parameters used to obtain 2-D images were as follows. The slice selection gradient (Z direction in Fig. 1) was 1.18×10^{-2} Tesla/meter, so the thickness of the potato slice excited by the gradient was 2.1 mm. The read out magnetic field gradient (Y direction in Fig. 1) was 1.00×10^{-2} Tesla/meter. The increment of the phase encoding gradient was 1.2×10^{-4} Tesla/meter. There were 64 phase encoding steps. More phase encoding steps will give better image resolution, but more time is required to collect each image. It took about 8 min to obtain each set of FID data.

The drying system was controlled so that the potato sample was dried with air at 60°C, 0.008 kgWater/kgAir absolute humidity, and 1.2 m/s velocity. The Sher-

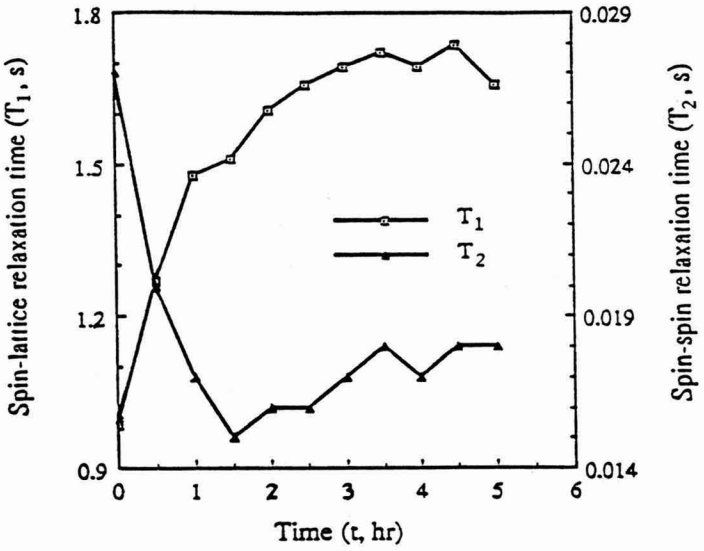

FIG. 3. SPIN-LATTICE RELAXATION TIME (T_1) AND SPIN-SPIN RELAXATION TIME (T_2) VERSUS TIME (t)

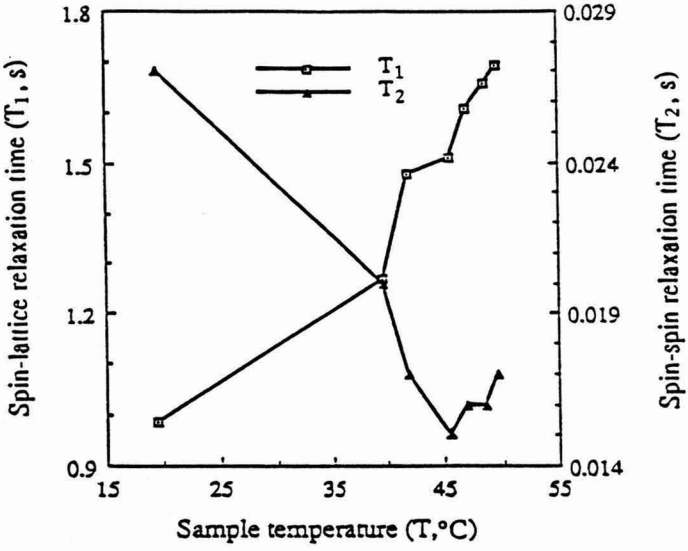

FIG. 4. SPIN-LATTICE RELAXATION TIME (T_1) AND SPIN-SPIN RELAXATION TIME (T_2) VERSUS SAMPLE TEMPERATURE (T)

wood number, which is the ratio of external to internal moisture transfer rates, was calculated and found to be much larger than 10.0. With the airflow rate of 1.2 m/s, a diffusivity of 7.28×10^{-6} m^2/s, and a mass conductivity of 0.295 m/s, the Sherwood number was 2.8×10^3. Therefore, the assumption of internal, not external, resistance to mass transfer was reasonable.

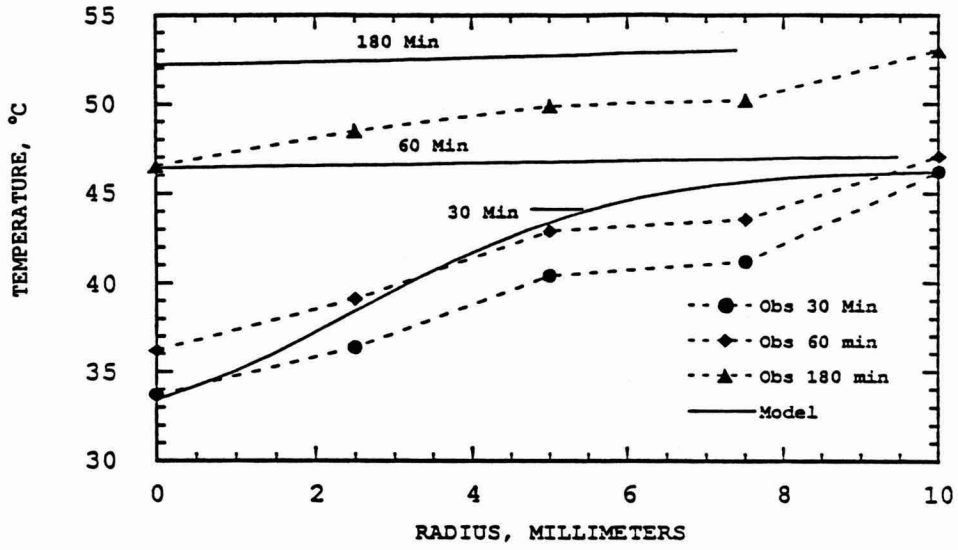

FIG. 5. TEMPERATURE PROFILES SIMULATED BY THE COUPLED MODEL AND OBSERVED IN THE SAMPLE DURING DRYING

The absorption tests were performed at room temperature at about 23°C. The initially dried sample was first set at room temperature to reach a uniform inside temperature profile before it was put into the tube of water for the absorption test.

For the water absorption experiments, the obtained proton density profiles were converted into moisture profiles by scaling the value of the proton density of pure water to 100% moisture. For drying experiments, the average MRI signal intensity of the samples at each different drying time was compared with the average moisture content of the sample obtained by oven drying method, to scale the moisture profiles obtained by the MRI. A sample for each condition was also cut into five concentric rings using sharp end pipes of 6, 8, 10, and 12 mm in diameter and 0.3 mm in wall thickness, and the moisture content of each ring was determined (103°C oven, 24 h). The scalings were verified by moisture profiles obtained with the oven drying of these concentric rings. The difference in the MRI and oven measurements was less than 3% moisture content. Although the ring-cutting technique is certainly inaccurate, there are not other accurate noninvasive methods to verify the MRI results. The converted moisture content data were input to a finite difference computer program, which solved equation (2) and minimized the difference (ERR) between the MRI and the oven moisture contents [$M(t,r_j)$'s in Eq. (3)], to determine the effective moisture diffusion coefficient, D.

The temperature profiles inside the potato cylinder were measured outside the MRI system at the same conditions as those used for the MRI experiment. Thermocouples were inserted in the potato cylinder, and temperature readings were taken at 30 min intervals (Fig. 5).

Prediction of Moisture and Temperature Profiles with a Coupled Model

A numerical model was written to simulate the transfer of moisture and heat through the sample. If the moisture diffusivity is allowed to vary spatially in the sample, the governing equation (Eq. 2) can be written as:

$$\frac{\partial M}{\partial t}=\frac{1}{r}\frac{\partial(Dr\frac{\partial M}{\partial r})}{\partial r} \tag{5}$$

For temperature diffusion, the governing equation can be written as:

$$\frac{\partial T}{\partial t}=\frac{1}{r}\frac{\partial(Kr\frac{\partial T}{\partial r})}{\partial r}-C_p\frac{\partial M}{\partial t} \tag{6}$$

where T is the temperature, C_p is the heat of vaporization of water (2385 KJ/KgH_2O), and K is the thermal diffusion coefficient.

Taylor series approximations to these equations provide the following one-dimensional, explicit (forward in time), centered in space numerical solutions.

For moisture diffusion, the equation is:

$$\begin{aligned} M(t+1,r_i) = {} & M(t,r_{i+1})[D_i\frac{\delta t}{\delta r^2}+D_i\frac{\delta t}{2r\delta r}+\frac{(D_{i+1}-D_{i-1})\delta t}{4\delta r^2}]+M(t,r_i)[1-2D_i\frac{\delta t}{\delta r^2}]+ \\ & M(t,r_{i-1})[D_i\frac{\delta t}{\delta r^2}-D_i\frac{\delta t}{2r\delta r}-\frac{(D_{i+1}-D_{i-1})\delta t}{4\delta r^2}] \end{aligned} \tag{7}$$

For temperature, the equation is:

$$\begin{aligned} T(t+1,r_i) = {} & T(t,r_{i+1})[K_i\frac{\delta t}{\delta r^2}+K_i\frac{\delta t}{2r\delta r}+\frac{(K_{i+1}-K_{i-1})\delta t}{4\delta r^2}]+T(t,r_i)[1-2K_i\frac{\delta t}{\delta r^2}]+ \\ & T(t,r_{i-1})[K_i\frac{\delta t}{\delta r^2}-K_i\frac{\delta t}{2r\delta r}-\frac{(K_{i+1}-K_{i-1})\delta t}{4\delta r^2}]-C_p(M(t,R)-M(t+1,R)) \end{aligned} \tag{8}$$

where δt is the model time step; δr is the model grid distance; subscripts i, i+1, and i-1 indicate the current grid point, the adjacent grid point toward the exterior of the sample, and the adjacent point toward interior of the sample, respectively; subscripts t and t+1 indicate the values at the beginning of the current time step and the values at the beginning of the next time step, respectively; M(R) is the moisture content of the grip at the surface of the sample. The term $C_p[M(t,R)-M(t+1,R)]$ is the means of coupling mass and heat transfer, as this term calculates the heat required to evaporate the moisture loss during each time step.

The model assumes axial symmetry, and simulates from the center of the sample along a radius to the edge of the sample. The model was used to simulate simultaneous heat and mass (moisture) transfer and shrinkage of the sample as a result of water loss. Boundary conditions for the model were (1) a zero flux for both heat and mass transfer at the center, and (2) the temperature obtained by the

couples and the equilibrium moisture content for the drying air at the external boundary.

The simulation procedure, for each time step, was to calculate moisture diffusion, then to calculate the moisture loss from the sample, and use this moisture loss to calculate the heat loss due to evaporation, and then calculate the heat transfer. Shrinkage was simulated by reducing the radius for each step based on the average rate measured from the sample during drying. These steps were repeated for each time step for the entire period of drying simulation.

An average shrinkage rate was estimated based on the reduction in radius of the sample over the entire period of drying. An average thermal diffusion coefficient was estimated by iterating different values of K to select an empirical best fit to the temperature gradient measured after 30 min of drying.

RESULTS AND DISCUSSION

Moisture Profiles—NMR Images

Two dimensional NMR proton density images of potato samples during drying and absorption are shown in Fig. 6 and 7 respectively, where intensity is proportional to moisture content. Figure 6, window 1 is a cross-sectional image of proton density in the potato cylinder before drying. Windows 2 through 8 show the

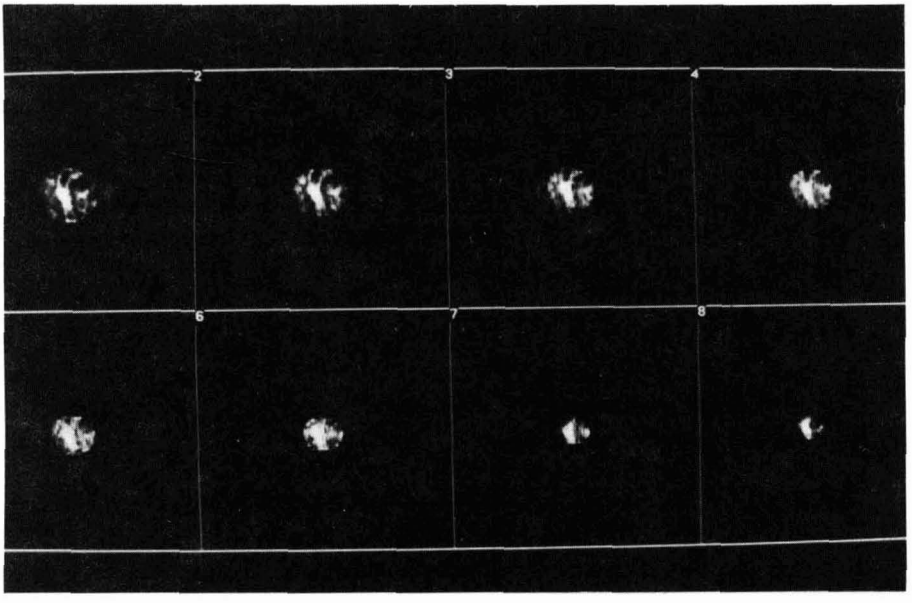

FIG. 6. NMR PROTON DENSITY IMAGES OF POTATO DURING DRYING (TIME STEP = 1 H)

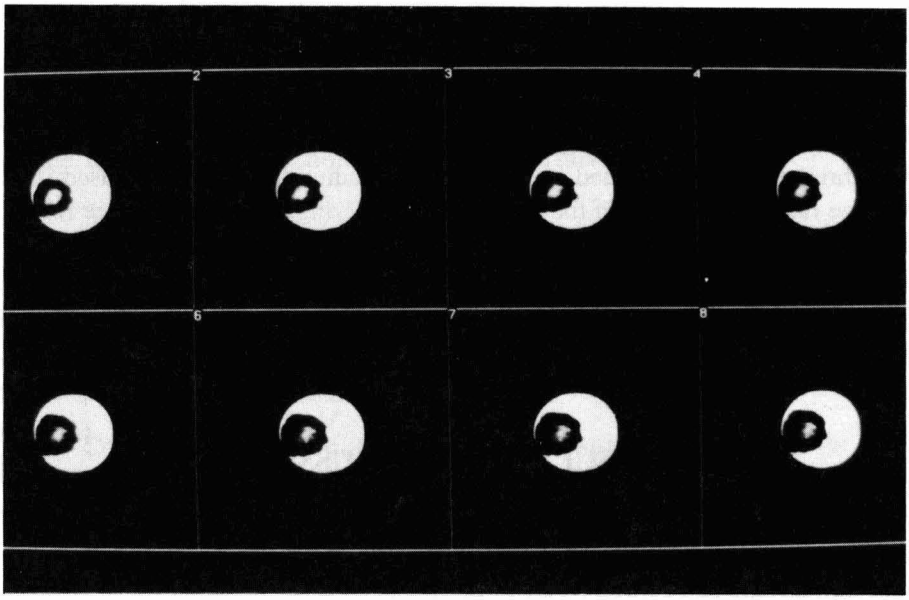

FIG. 7. NMR PROTON DENSITY IMAGES OF POTATO DURING ABSORPTION (TIME STEP = 1 H)

proton density in the same cross section at 60 min intervals during drying at 60°C. The initial moisture distribution was not uniform inside the potato. As the drying proceeded, the sample shrunk, and the moisture distribution became more uniform as the moisture decreased. The observed moisture profiles did not follow the theoretical curve predicted by Fick's law, but tended low and a uniform gradient inside the sample with a sharp gradient at the interface with the air. These results may be caused by (1) lower diffusivities at lower moisture contents and (2) case hardening of the outer surface with an increased resistance to mass transfer. Figure 7, windows 1 through 8 show the proton density images in a cross section at 60 min intervals during absorption at 23°C.

The contour images with the moisture profiles in the potato after 60 min of drying and 60 min of absorption are shown in Fig. 8. Each contour stands for a constant moisture content line in the sample, the actual value of these lines can be found from the corresponding points in the moisture profile for an axis through the center of the sample shown right above the contour image in Fig. 8. The one-dimensional moisture distribution profiles of the potato cylinder obtained from the imaging system during drying and absorption are shown in Fig. 9, from which the moisture distribution of the potato during drying and absorption can be compared at different times and at different radial positions. The shrinkage during drying and expansion during absorption may be measured from Fig. 6 and 9.

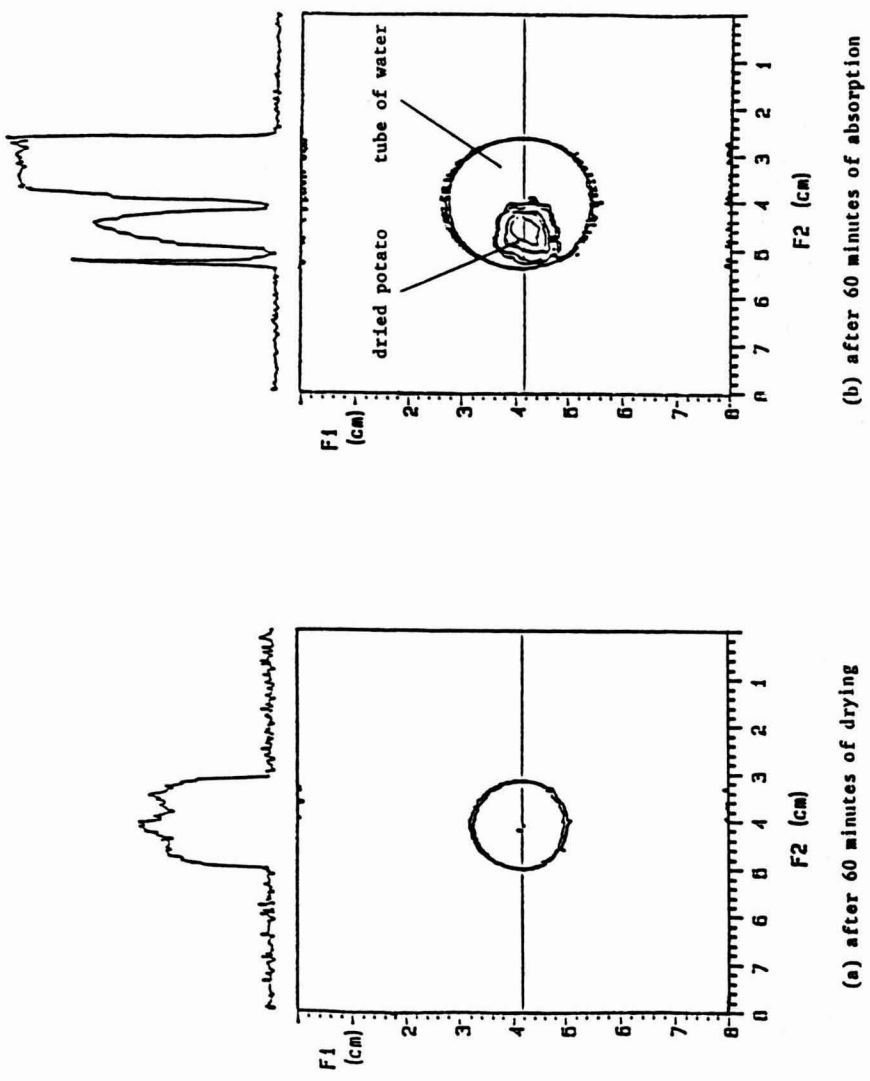

FIG. 8. NMR PROTON DENSITY CONTOUR IMAGES WITH MOISTURE PROFILES FOR A LINE THROUGH THE CENTER OF THE SAMPLE
(a) after 60 min of drying and (b) after 60 min of absorption.

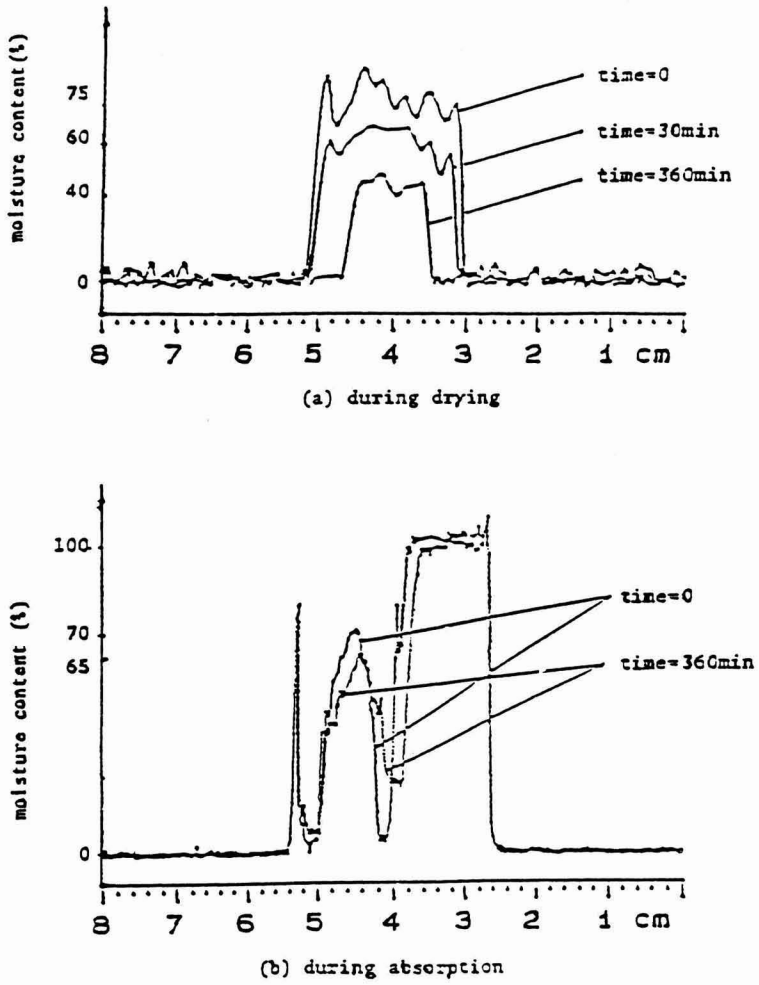

FIG. 9. MRI MOISTURE PROFILES DURING DRYING AND ABSORPTION

Figures 6 and 9(a) show that at the beginning of drying the moisture movement was very fast, while toward the middle and end of drying the movement was much slower. For example, it took only 30 min for the moisture content to drop from 75% to 60%, but it took 360 min for the moisture content to drop from 60% to 45%.

Comparing Fig. 8(b) with 8(a), it was found that the rate of absorption for the dried potato was much lower than the drying rate of the fresh potato. The hard layer produced during the drying process served as a barrier for moisture absorption. In turn, the volume expansion was very slow and small due to the structural changes in the hard layer.

Moisture Diffusivities

The effective diffusivity data were modeled as an exponential function of mean moisture content, using a least squares fit. The expressions obtained effective moisture diffusion coefficient (m^2/s) for during drying and absorption, respectively, were

$$D = 5.128 \times 10^{-13} e^{0.135M} \quad \text{for drying at 40°C} \quad (9)$$

$$D = 2.805 \times 10^{-16} e^{0.187M} \quad \text{for absorption at 23°C} \quad (10)$$

where M is the mean moisture content (%, wb). The squares of the correlation coefficient, r^2, were 0.96 and 0.99 for Eq. (9) and (10) respectively. These diffusivities give best fit for a mean moisture content of the sample, averaged in the radial direction. The effective moisture diffusion coefficient versus average moisture content for drying with a sample temperature of 40°C and for absorption at 23°C are shown in Fig. 10. With high resolution moisture and temperature profiles, and a better conceptional model of mass transfer, this method can also be used to map the actual transport coefficient data inside the sample.

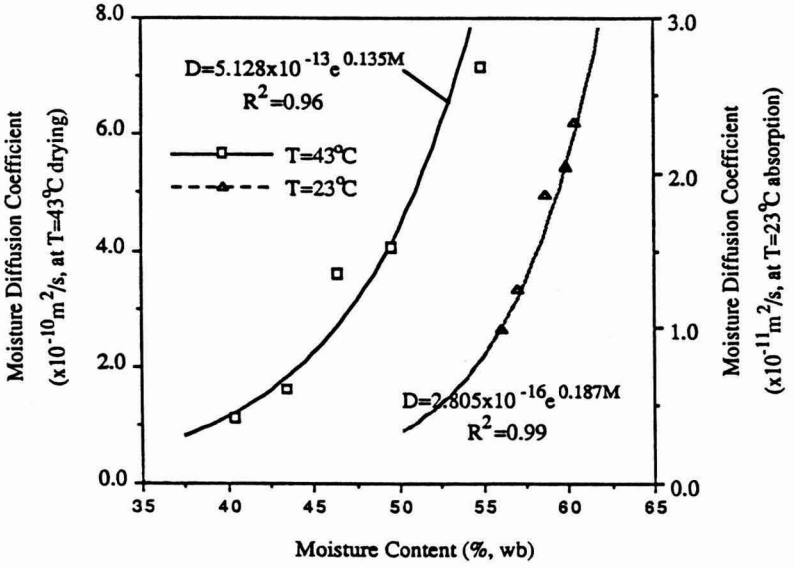

FIG. 10. MOISTURE DIFFUSION COEFFICIENT VERSUS MOISTURE CONTENT

Chirife (1983) reported the diffusivity in a potato during drying as $D = 1.0 \times 10^{-10}$ m^2/s, at a 65°C sample temperature and for moisture contents less than 15%. The results we obtained, $D = 1.04 \times 10^{-10}$ to 7.28×10^{-10} m^2/s for moisture contents from 40–55% at a sample temperature of 40°C, appeared reasonable in comparison. Differences might be due to the lower temperature and higher moisture contents used in the present study.

We have not found data for the moisture diffusion coefficient during absorption, but there are results for similar material, such as for floury endosperm of corn, $D = 1.767 \times 10^{-11} e^{0.086M}$ (m^2/s) (Syarief *et al.* 1987). For a moisture content of 60%, the moisture diffusion coefficient predicted by the equation for corn endosperm is 3.08×10^{-9} m^2/s. At the same moisture, the potato diffusivity was 2.33×10^{-11} m^2/s. The difference may be because the model for corn endosperm is only valid for low moisture contents, below 25%, and the structure of the floury endosperm is different from the potato.

Predicted Results from the Coupled Model

Simulation results from the coupled model indicate that the Fickian diffusion equation does not adequately predict temperature and moisture movement through

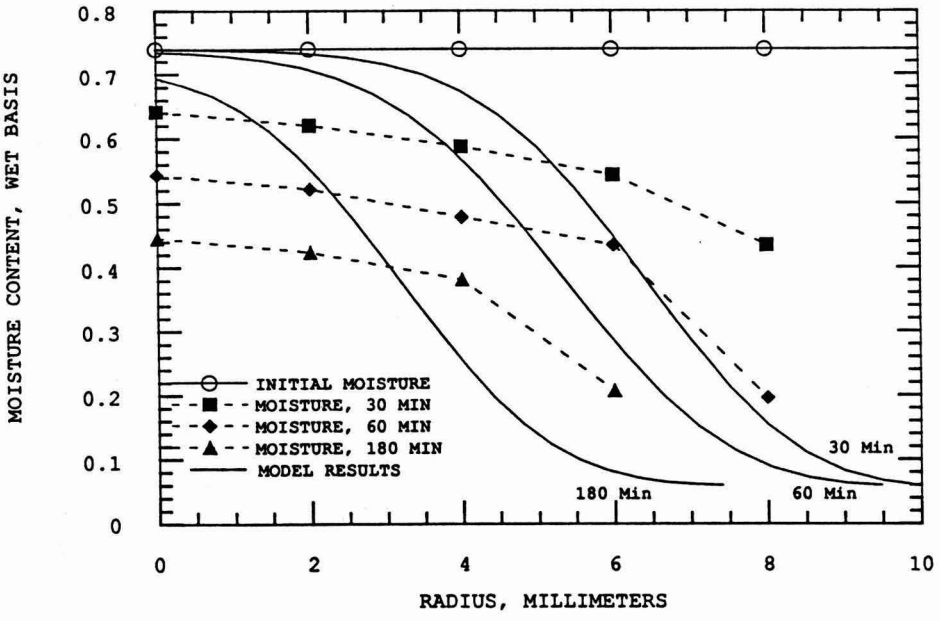

FIG. 11. SHRINKAGE SIMULATED AS CONSTANT RATE AND OBSERVED IN THE SAMPLE DURING DRYING

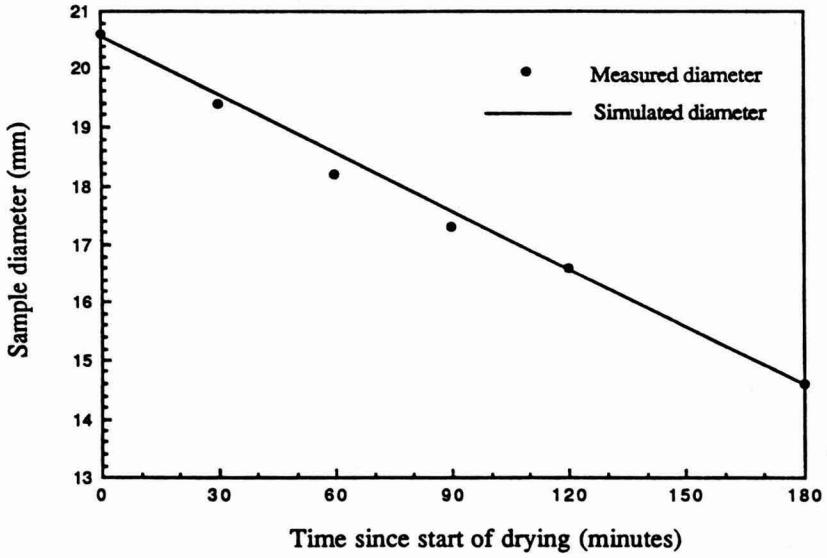

FIG. 12. MOISTURE CONTENT SIMULATED WITH CONSTANT-RATE SHRINKAGE MODEL AND OBSERVED IN THE SAMPLE DURING DRYING

the sample during drying. Simulated and observed temperature profiles (Fig. 5) indicate that the model, with a constant thermal diffusion coefficient of 3.2×10^{-9} m^2/s underestimates heat transfer at the early stage of the simulation, but overpredicts heat transfer as the simulation progresses.

Shrinkage was simulated as occurring at the average rate observed from the sample by MRI (2.75×10^{-7} m/s). Simulated and observed shrinkage of the sample are shown in Fig. 11. Moisture profiles from this simulation and from MRI images of the sample are shown in Fig. 12. The MR images show greater moisture contents near the edge of the sample than the simulated profiles, while the average simulated moisture content agrees with that observed.

Some of the reasons why the moisture profiles predicted by the model were steeper than the ones obtained by the NMR images (Fig. 12) might be: (1) the different procedure used to estimate the moisture diffusion coefficients in the model, the coupled model estimated moisture movement through the sample using moisture diffusion coefficients from Eq. (9) as local diffusion coefficients, however, Eq. (9) estimated the effective diffusion coefficient for the entire sample at a mean moisture content; (2) the temperature dropped dramatically for the drying air near the surface of the sample according to the temperature profile obtained by the thermocouples, this surface boundary layer was not considered in the model; (3) the coupled model did not account for changes in the moisture diffusion coefficient due to case hardening at the sample; and (4) the temperature gradient, although very small, that did exist in the sample. Therefore, shrinkage, case hardening, and boundary layer studies are needed to further understand these transport processes.

SUMMARY AND CONCLUSIONS

A new method using nuclear magnetic resonance imaging was developed to determine the transient moisture profiles and effective moisture diffusion coefficient values for a potato during drying and absorption. The determination of the moisture diffusion coefficient was based on NMR images of moisture distribution during drying and absorption and on numerical modeling of the diffusion process.

REFERENCES

BELL, R.A. 1986. Other horizons in NMR. Syllabus of the Santa Fe NMR Workshop.

BLACKLAND, S. and MANSFIELD, P. 1986. Diffusion in liquid-solid systems by NMR imaging. J. Phys. C: Solid State Phys. *19*, L49–L52.

CALLAGHAN, P.T. and ECCLES, C.D. 1979. Diffusion of fat and water in cheese as studied by pulses gradient nuclear magnetic resonance. J. Colloid Interface Sci. *93*(2), 521.

CHEN, P., McCARTHY, M.J. and KAUTEN, R. 1989. NMR for internal quality evaluation of fruits and vegetables. Trans. ASAE *32*(5), 1747–1753.

CHIRIFE, J. 1983. Fundamentals of drying mechanism during air dehydration of foods. In *Advances in Drying*, Vol. 2, (A.S. Mujumder, ed.) Hemisphere Publishing, Washington, D.C.

CHU, S.T. and HUSTRULID, A. 1968. General characteristics of variable diffusivity process and the dynamic equilibrium moisture content. Trans. ASAE *11*(5), 709–710, 715.

CRANK, J. and PARK, G.S. 1976. Diffusion in polymers, 2nd ed., Academic Press, New York.

GUILLOT, G., TROKINER, A., DARRASSE, L., and SAINT-JALMES, H., 1989. Drying of a porous rock monitored by NMR imaging. J. Phys. D: Appl. Phys. *22*, 1646–1649.

HEIL, J.R., PERKINS, W.E. and McCARTHY, M.J. 1990. Use of magnetic resonance procedures for measurement of oil in french-style dressings. J. Food Sci. *55*(3), 763.

JENNER, C.F., XIA, Y., ECCLES, C.D. and CALLAGHAN, P.T. 1988. Circulation of water within wheat grain revealed by nuclear magnetic resonance microimaging. Nature *336*, 399–402.

KASHKINA, L.V. 1979. Proton magnetic resonance study of properties of water absorbed on starch. Colloid J. USSR *41*, 368.

LAUTERBUR, P.C. 1986. New techniques in NMR zeugmatographic imaging. Biomed. Imaging 97–106.

LOMAURO, G.J. and BAKSHI, A.S. 1985. Finite element analysis of moisture diffusion in stored foods. J. Food Sci. *50*.

McCARTHY, M.J. 1990. Interpretation of the magnetic resonance imaging signal from a foam. AICHE J. *36*(2), 287–290.

McCARTHY, M.J. and PEREZ, E. 1989. Measurement of effective moisture diffusivities using magnetic resonance imaging. Proceedings of the Fifth International Congress on Engineering and Food, Germany.

MEYER, R.A. and BROWN, T.R. 1988. Diffusion measurements by NMR imaging. J. Magnetic Resonance. *76.*

PEREZ, E., KAUTEN, R. and McCARTHY, M.J. 1988. Nondestructive measurement of moisture profiles during the drying of an apple. Presented at the Annual Meeting of IFT.

ROTHWELL, W.P., HOLECEK, D.R. and KERSHAW, J.A. 1984. NMR images: study of fluid absorption by polymer composites. J. Polym. Sci, Polym. Lett. Ed. *22*, 241–247.

RUAN, R. and LITCHFIELD, J.B. 1989. Magnetic resonance imaging technology and development of an NMR imaging probe for food materials. ASAE Winter Meeting, New Orleans, LA. Paper No. 893549.

SONG, H. and LITCHFIELD, J.B. 1990. Nondestructive measurement of transient moisture profiles in corn during drying using NMR imaging. Trans. ASAE *33*(4), 1286–1290.

SONG, H., RUAN, R. and LITCHFIELD, J.B. 1990. Microscopic, 3-D measurements of foods during drying using magnetic resonance imaging. Proceeding of 1990 Food Processing Automation Conference, Lexington, Kentucky.

STARK, D.D. and BRADLEY, W.G. 1988. Magnetic resonance imaging. The C. V. Mosby Company.

SYRIEF, A.M., GUSTFSON, R.J. and MOREY, R.V. 1987. Moisture diffusion coefficients for yellow-dent corn components. Trans. ASAE *30*(2), 522–528.

WELTY, J.R., WICKS, C.E. and WILSON, R.E. 1984. Fundamental of momentum, heat, and mass transfer. John Wiley & Sons, New York.

ZHOU, X., POTTER, C.S., LAUTERBUR, P.C. and VOTH, B. 1989. 3D microscopic NMR imaging with $(6.37\ \mu m)^3$ isotropic resolution. SMRM 8th Annual Meeting. Amsterdam, The Netherlands.

AUTHOR INDEX

Journal of Food Process Engineering **14** (1991) 315-317.

SUBJECT INDEX

Journal of Food Process Engineering *14(1991) 319–320. All Rights Reserved.*

F
N
P

PUBLICATIONS IN FOOD SCIENCE AND NUTRITION

Journals

JOURNAL OF MUSCLE FOODS, N.G. Marriott and G.J. Flick, Jr.
JOURNAL OF SENSORY STUDIES, M.C. Gacula, Jr.
JOURNAL OF FOOD SERVICE SYSTEMS, O.P. Snyder, Jr.
JOURNAL OF FOOD BIOCHEMISTRY, J.R. Whitaker, N.F. Haard and H. Swaisgood
JOURNAL OF FOOD PROCESS ENGINEERING, D.R. Heldman and R.P. Singh
JOURNAL OF FOOD PROCESSING AND PRESERVATION, D.B. Lund
JOURNAL OF FOOD QUALITY, R.L. Shewfelt
JOURNAL OF FOOD SAFETY, T.J. Montville and A.J. Miller
JOURNAL OF TEXTURE STUDIES, M.C. Bourne and P. Sherman

Books

NUTRIENT ADDITIONS TO FOOD, J.C. Bauernfeind and P.A. Lachance
NITRITE-CURED MEAT, R.G. Cassens
THE POTENTIAL FOR NUTRITIONAL MODULATION OF THE AGING PROCESSES, D.K. Ingram *et al.*
CONTROLLED/MODIFIED ATMOSPHERE/VACUUM PACKAGING OF FOODS, A.L. Brody
NUTRITIONAL STATUS ASSESSMENT OF THE INDIVIDUAL, G.E. Livingston
QUALITY ASSURANCE OF FOODS, J.E. Stauffer
THE SCIENCE OF MEAT AND MEAT PRODUCTS, 3RD ED., J.F. Price and B.S. Schweigert
HANDBOOK OF FOOD COLORANT PATENTS, F.J. Francis
ROLE OF CHEMISTRY IN THE QUALITY OF PROCESSED FOODS, O.R. Fennema, W.H. Chang and C.Y. Lii
NEW DIRECTIONS FOR PRODUCT TESTING AND SENSORY ANALYSIS OF FOODS, H.R. Moskowitz
PRODUCT TESTING AND SENSORY EVALUATION OF FOODS, H.R. Moskowitz
ENVIRONMENTAL ASPECTS OF CANCER: ROLE OF MACRO AND MICRO COMPONENTS OF FOODS, E.L. Wynder *et al.*
FOOD PRODUCT DEVELOPMENT IN IMPLEMENTING DIETARY GUIDELINES, G.E. Livingston, R.J. Moshy, and C.M. Chang
SHELF-LIFE DATING OF FOODS, T.P. Labuza
RECENT ADVANCES IN OBESITY RESEARCH, VOL. V, E. Berry *et al.*
RECENT ADVANCES IN OBESITY RESEARCH, VOL. IV, J. Hirsch *et al.*
RECENT ADVANCES IN OBESITY RESEARCH, VOL. III, P. Bjorntorp *et al.*
RECENT ADVANCES IN OBESITY RESEARCH, VOL. II, G.A. Bray
RECENT ADVANCES IN OBESITY RESEARCH, VOL. I, A.N. Howard
ANTINUTRIENTS AND NATURAL TOXICANTS IN FOOD, R.L. Ory
UTILIZATION OF PROTEIN RESOURCES, D.W. Stanley *et al.*
VITAMIN B_6: METABOLISM AND ROLE IN GROWTH, G.P. Tryfiates
FOOD POISONING AND FOOD HYGIENE, 4TH ED., B.C. Hobbs *et al.*
POSTHARVEST BIOLOGY AND BIOTECHNOLOGY, H.O. Hultin and M. Milner

Newsletters

MICROWAVES AND FOOD, R.V. Decareau
FOOD INDUSTRY REPORT, G.C. Melson
FOOD, NUTRITION AND HEALTH, P.A. Lachance and M.C. Fisher
FOOD PACKAGING AND LABELING, S. Sacharow

U.S. Postal Service

STATEMENT OF OWNERSHIP, MANAGEMENT AND CIRCULATION

Required by 39 U.S.C. 3685)

1A. Title of Publication	1B. PUBLICATION NO.	2. Date of Filing
JOURNAL OF FOOD PROCESS ENGINEERING	0 1 4 5 8 8 7 6	Oct. 1, 1991
3. Frequency of Issue	3A. No. of Issues Published Annually	3B. Annual Subscription Price
Quarterly	4	$104.00

4. Complete Mailing Address of Known Office of Publication *(Street, City, County, State and ZIP+4 Code) (Not printers)*

2 Corporate Dr., POB 374, Trumbull, Fairfield, CT 06611

5. Complete Mailing Address of the Headquarters of General Business Offices of the Publisher *(Not printer)*

2 Corporate Dr., POB 374, Trumbull, CT 06611

6. Full Names and Complete Mailing Address of Publisher, Editor, and Managing Editor *(This item MUST NOT be blank)*

Publisher *(Name and Complete Mailing Address)*

John J. O'Neil, 2 Corporate Dr., POB 374, Trumbull, CT 06611

Editor *(Name and Complete Mailing Address)*

Dr. Dennis R. Heldman, 83 Gordon Avenue, Lawrenceville, NJ 08648

Editor *(Name and Complete Mailing Address)*

Dr. R. Paul Singh, Univ. of California, Dept. of Agricultural Eng., Davis, CA 95616

7. Owner *(If owned by a corporation, its name and address must be stated and also immediately thereunder the names and addresses of stockholders owning or holding 1 percent or more of total amount of stock. If not owned by a corporation, the names and addresses of the individual owners must be given. If owned by a partnership or other unincorporated firm, its name and address, as well as that of each individual must be given. If the publication is published by a nonprofit organization, its name and address must be stated.) (Item must be completed.)*

Full Name	Complete Mailing Address
Food & Nutrition Press, Inc.	2 Corporate Dr., POB 374, Trumbull, CT 06611
John J. O'Neil	53 Stonehouse Rd., Trumbull, CT 06611
Michael J. Tully	3 N.Slope,Union Gap Village, Clinton, NJ 08809
Kathryn O. & Christopher R. Ziko	8 Maria Alicia Dr., Huntington, CT 06484
John J.O'Neil, Jr.	115 Maureen St., Stratford, CT 06497

8. Known Bondholders, Mortgagees, and Other Security Holders Owning or Holding 1 Percent or More of Total Amount of Bonds, Mortgages or Other Securities *(If there are none, so state)*

Full Name	Complete Mailing Address
None	

9. For Completion by Nonprofit Organizations Authorized To Mail at Special Rates *(DMM Section 423.12 only)*
The purpose, function, and nonprofit status of this organization and the exempt status for Federal income tax purposes *(Check one)*

☐ (1) Has Not Changed During Preceding 12 Months ☐ (2) Has Changed During Preceding 12 Months

(If changed, publisher must submit explanation of change with this statement.)

10. Extent and Nature of Circulation *(See instructions on reverse side)*	Average No. Copies Each Issue During Preceding 12 Months	Actual No. Copies of Single Issue Published Nearest to Filing Date
A. Total No. Copies *(Net Press Run)*	417	400
B. Paid and/or Requested Circulation 1. Sales through dealers and carriers, street vendors and counter sales	0	0
2. Mail Subscription *(Paid and/or requested)*	207	183
C. Total Paid and/or Requested Circulation *(Sum of 10B1 and 10B2)*	207	183
D. Free Distribution by Mail, Carrier or Other Means Samples, Complimentary, and Other Free Copies	49	53
E. Total Distribution *(Sum of C and D)*	256	236
F. Copies Not Distributed 1. Office use, left over, unaccounted, spoiled after printing	161	164
2. Return from News Agents	0	0
G. TOTAL *(Sum of E, F1 and 2—should equal net press run shown in A)*	417	400

11. I certify that the statements made by me above are correct and complete

Signature and Title of Editor, Publisher, Business Manager, or Owner

PS Form **3526**, Dec. 1987 *(See instructions on reverse)*

GUIDE FOR AUTHORS

Typewritten manuscripts in triplicate should be submitted to the editorial office. The typing should be double-spaced throughout with one-inch margins on all sides.

Page one should contain: the title, which should be concise and informative; the complete name(s) of the author(s); affiliation of the author(s); a running title of 40 characters or less; and the name and mail address to whom correspondence should be sent.

Page two should contain an abstract of not more than 150 words. This abstract should be intelligible by itself.

The main text should begin on page three and will ordinarily have the following arrangement:

Introduction: This should be brief and state the reason for the work in relation to the field. It should indicate what new contribution is made by the work described.

Materials and Methods: Enough information should be provided to allow other investigators to repeat the work. Avoid repeating the details of procedures which have already been published elsewhere.

Results: The results should be presented as concisely as possible. Do not use tables *and* figures for presentation of the same data.

Discussion: The discussion section should be used for the interpretation of results. The results should not be repeated.

In some cases it might be desirable to combine results and discussion sections.

References: References should be given in the text by the surname of the authors and the year. *Et al.* should be used in the text when there are more than two authors. All authors should be given in the Reference section. In the Reference section the references should be listed alphabetically. See below for style to be used.

DEWALD, B., DULANEY, J.T., and TOUSTER, O. 1974. Solubilization and polyacrylamide gel electrophoresis of membrane enzymes with detergents. In *Methods in Enzymology,* Vol. xxxii, (S. Fleischer and L. Packer, eds.) pp. 82–91, Academic Press, New York.

HASSON, E.P. and LATIES, G.G. 1976. Separation and characterization of potato lipid acylhydrolases. Plant Physiol. *57,*142–147.

ZABORSKY, O. 1973. *Immobilized Enzymes,* pp. 28–46, CRC Press, Cleveland, Ohio.

Journal abbreviations should follow those used in *Chemical Abstracts.* Responsibility for the accuracy of citations rests entirely with the author(s). References to papers in press should indicate the name of the journal and should only be used for papers that have been accepted for publication. Submitted papers should be referred to by such terms as "unpublished observations" or "private communication." However, these last should be used only when absolutely necessary.

Tables should be numbered consecutively with Arabic numerals. The title of the table should appear as below:

Table 1. Activity of potato acyl-hydrolases on neutral lipids, galactolipids, and phospholipids

Description of experimental work or explanation of symbols should go below the table proper. Type tables neatly and correctly as tables are considered art and are not typeset. Single-space tables.

Figures should be listed in order in the text using Arabic numbers. Figure legends should be typed on a separate page. Figures and tables should be intelligible without reference to the text. Authors should indicate where the tables and figures should be placed in the text. Photographs must be supplied as glossy black and white prints. Line diagrams should be drawn with black waterproof ink on white paper or board. The lettering should be of such a size that it is easily legible after reduction. Each diagram and photograph should be clearly labeled on the reverse side with the name(s) of author(s), and title of paper. When not obvious, each photograph and diagram should be labeled on the back to show the top of the photograph or diagram.

Acknowledgments: Acknowledgments should be listed on a separate page.

Short notes will be published where the information is deemed sufficiently important to warrant rapid publication. The format for short papers may be similar to that for regular papers but more concisely written. Short notes may be of a less general nature and written principally for specialists in the particular area with which the manuscript is dealing. Manuscripts which do not meet the requirement of importance and necessity for rapid publication will, after notification of the author(s), be treated as regular papers. Regular papers may be very short.

Standard nomenclature as used in the engineering literature should be followed. Avoid laboratory jargon. If abbreviations or trade names are used, define the material or compound the first time that it is mentioned.

EDITORIAL OFFICES: DR. D.R. HELDMAN, COEDITOR, *Journal of Food Process Engineering,* National Food Processors Association, 1401 New York Avenue, N.W., Washington, D.C. 20005 USA; or DR. R.P. SINGH, COEDITOR, *Journal of Food Process Engineering,* University of California, Davis, Department of Agricultural Engineering, Davis, CA 95616 USA.

CONTENTS